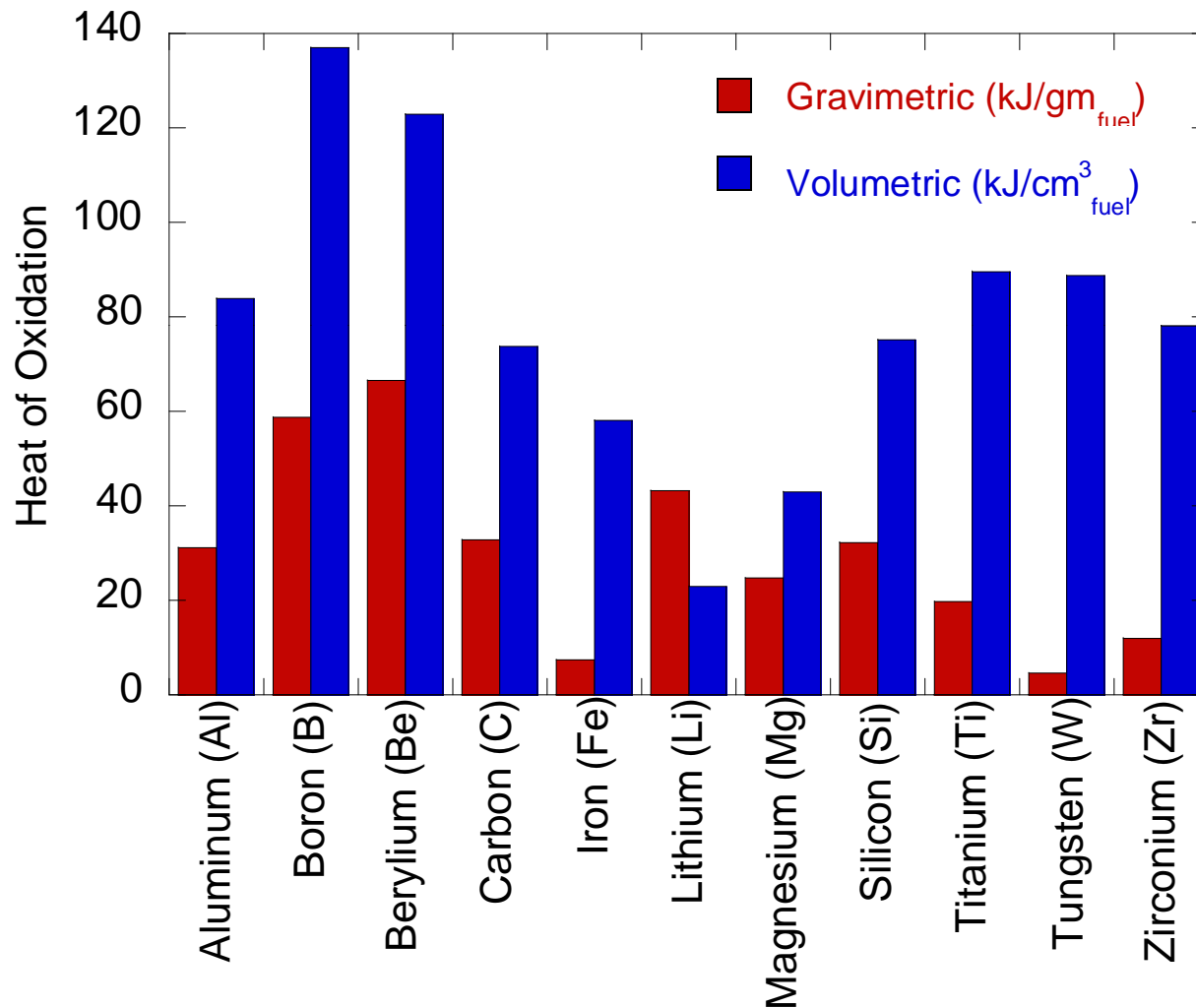5

Combustion of Energetic Materials

Richard A. Yetter

Penn State University

Princeton-Combustion Institute
2018 Summer School on Combustion
June 25-29, 2018
Princeton, NJ

Metal Combustion

Heats of Oxidation of Several Materials

Thermodynamic Considerations

- The determination of which metals will burn in the vapor phase or heterogeneously can be made from knowledge of the thermodynamic and physical properties of the metal and its oxide product.

- For oxygen containing environments, early studies (Glassman, Von Grosse and Conway) recognized
  - The importance of the volatility of the metal vs the metal oxide
  - The relationship between the energy required to gasify the metal or metal oxide and the overall energy available from the oxidation reaction – a limiting flame temperature

$$\Delta H_{vap\text{-}dissoc} > Q_R - (H^o_{T,vol} - H^o_{298}) = \Delta H_{avail}$$

Q_R = heat of reaction

$(H^o_{T,vol} - H^o_{298})$ = enthalpy required to raise the product oxide to its volatilization temperature

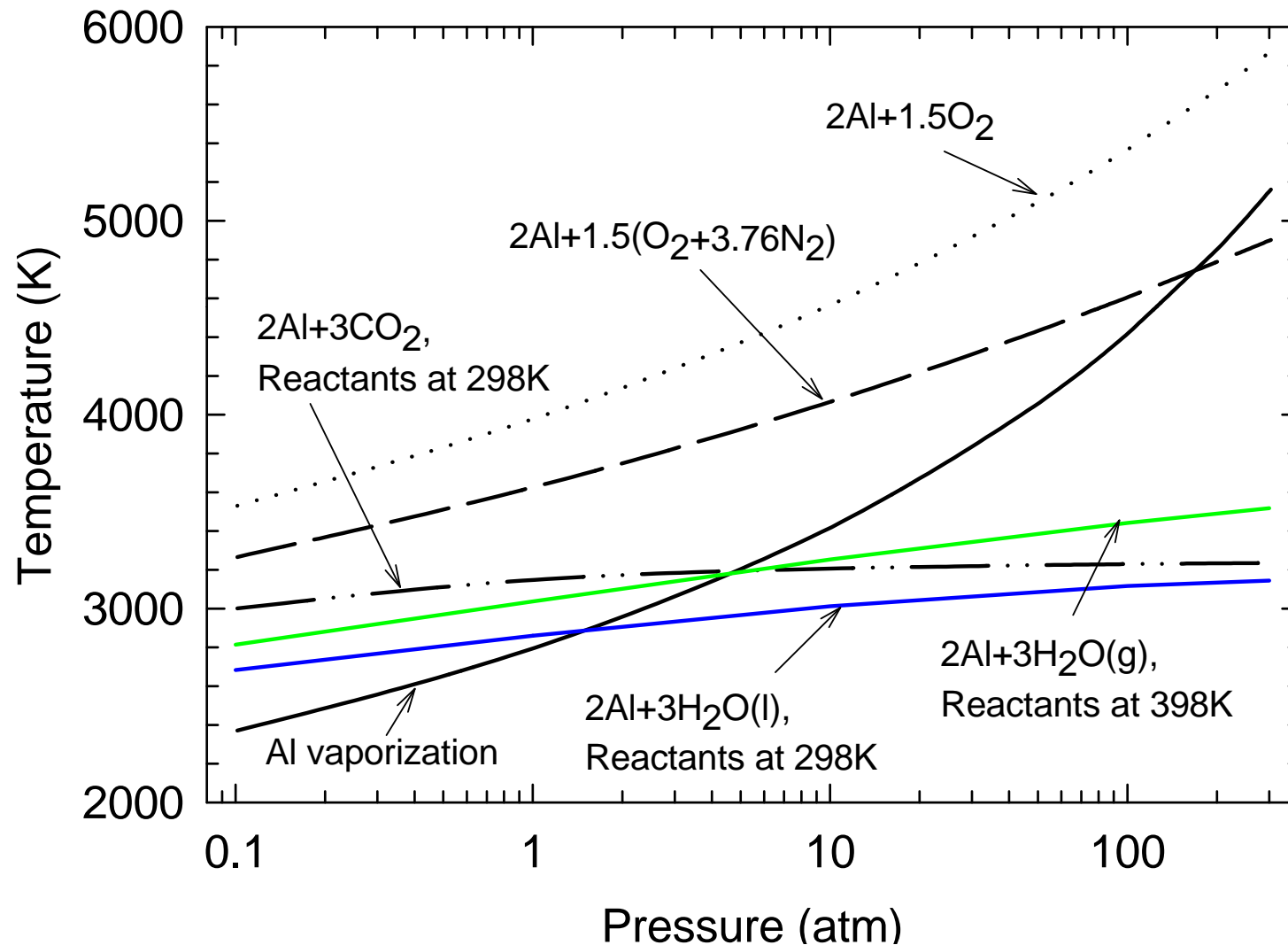$\Delta H_{vap\text{-}dissoc}$ = heat of vaporization-dissociation

Thermodynamic Considerations – Oxides

Metal	T_{bp} (K)	Oxide	T_{vol} (K)	$\Delta H_{f,298}$ (kJ/mol)	ΔH_{vol} (kJ/mol)	H_{Tvol}-H_{298} + ΔH_{vol} (kJ/mol)
Al	2791	Al_2O_3	4000	-1676	1860	2550
B	4139	B_2O_3	2130	-1272	360	640
Be	2741	BeO	4200	-608	740	1060
Cr	2952	Cr_2O_3	3280	-1135	1160	1700
Fe	3133	FeO	3400	-272	610	830
Hf	4876	HfO_2	5050	-1088	1014	1420
Li	1620	Li_2O	2710	-599	400	680
Mg	1366	MgO	3430	-601	670	920
Si	3173	SiO_2	2860	-904	606	838
Ti	3631	Ti_3O_5	4000	-2459	1890	2970
Zr	4703	ZrO_2	4280	-1097	920	1320

Glassman, Combustion, Academic Press, 3rd Edition, 1996

Classification of Metal Combustion

I	Volatile Product				Nonvolatile Product			
II	Volatile metal Gas-phase combustion		Nonvolatile metal Surface combustion		Volatile Metal Gas-phase combustion		Nonvolatile Metal Surface or condensed phase combustion	
III	Soluble	Nonsoluble	Soluble	Nonsoluble	Soluble	Nonsoluble	Soluble	Nonsoluble
	Product may dilute metal during burning and cause disruption if its BP exceeds that of metal	No flux of product to metal	Product may build up in metal during burning	No product penetration into metal	If product returns to metal it may dilute it and cause disruption	Disruption strongly favored if product returns to metal	Metal may diffuse through growing product layer, purely condensed phase combustion possible	Product coating makes ignition difficult

F.A. Williams, "Some Aspects of Metal Particle Combustion," Physical and Chemical Aspects of Combustion: A Tribute to Irv Glassman, F.L. Dryer and R.F. Sawyer, eds., Gordon and Breach, The Netherlands, 1997, pp. 267-289.

Thermodynamic Considerations – Effect of Pressure and Oxidizer

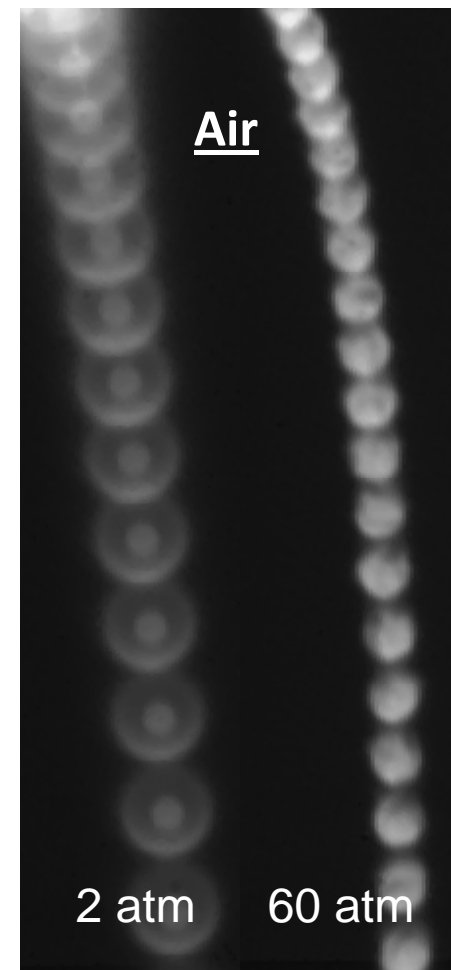Glassman and Yetter, Combustion, Academic Press, 4th Edition, 2008

Micron Aluminum Particle Combustion

Oxidizer Effects

Pressure Effects

R.A. Yetter and F.L. Dryer, in Fire in Free Fall: Microgravity Combustion, H. Ross, Ed., Academic Press, Chapter 6, 2001.
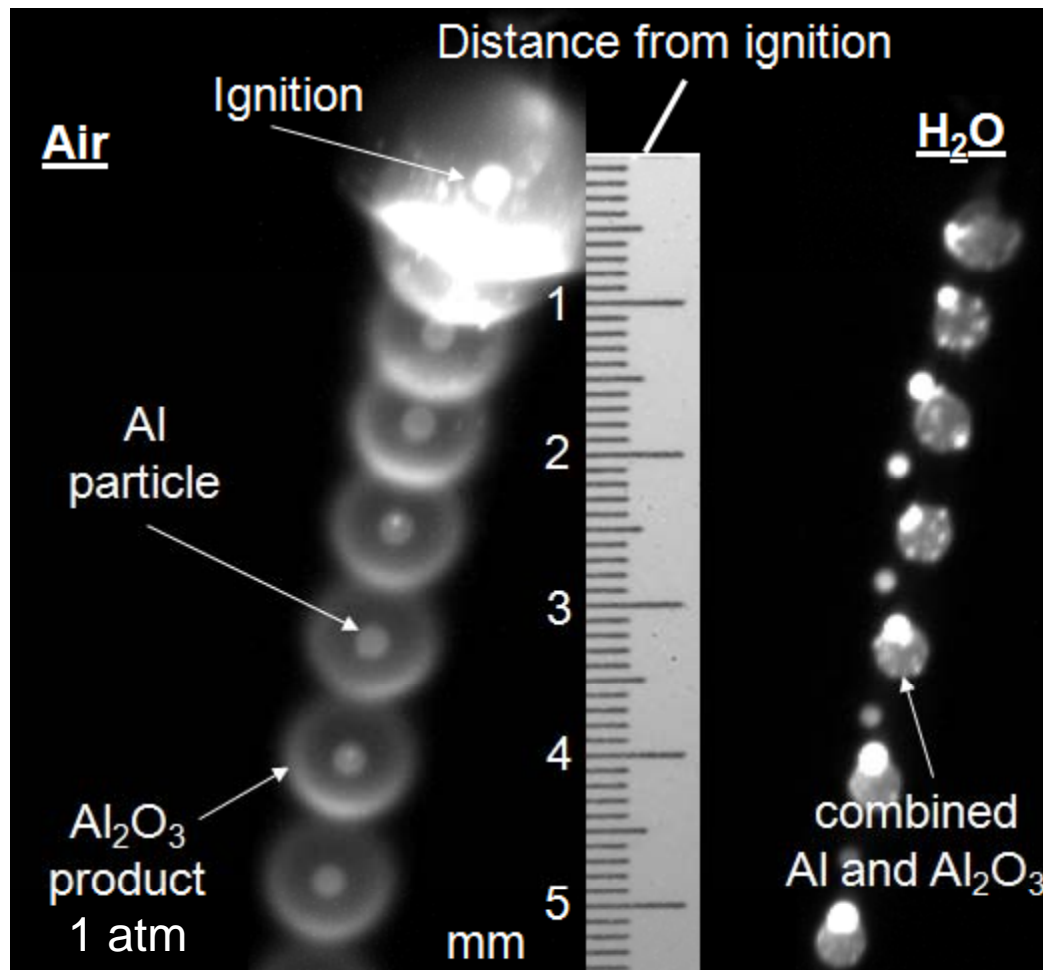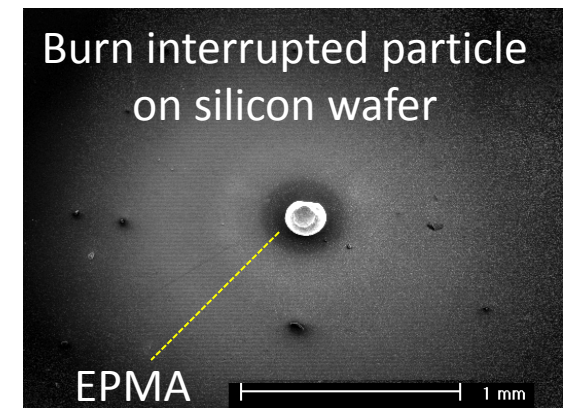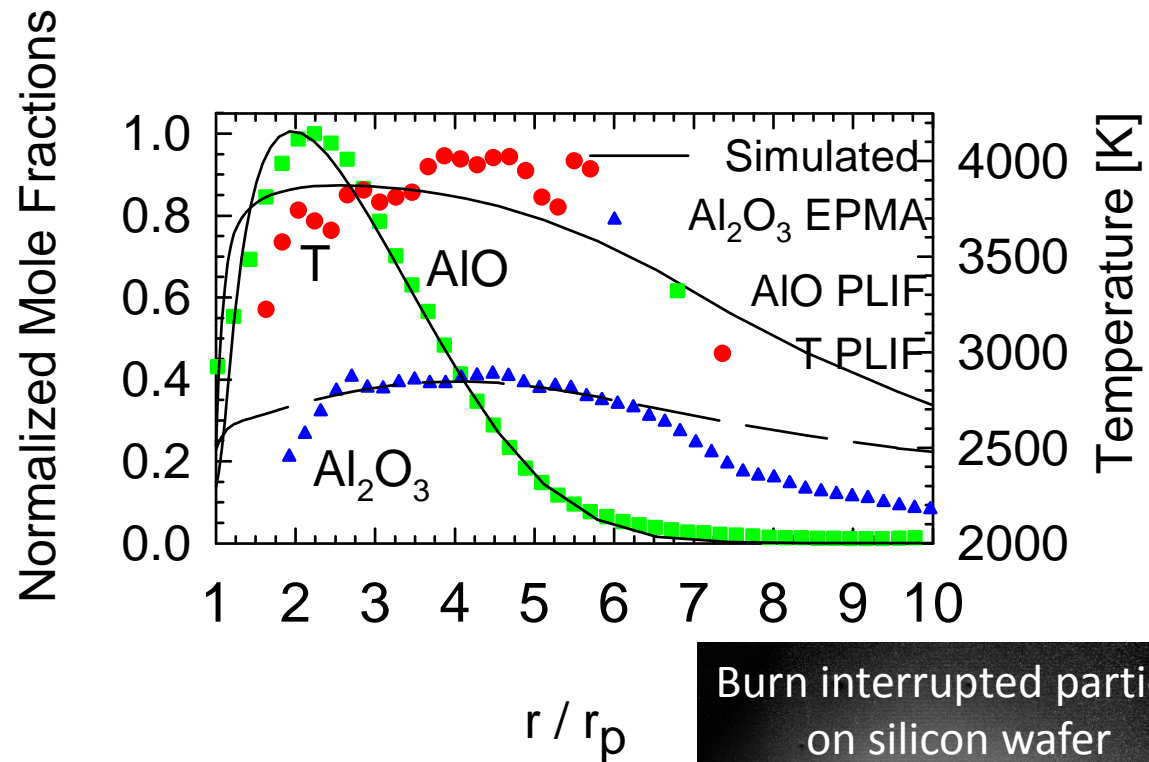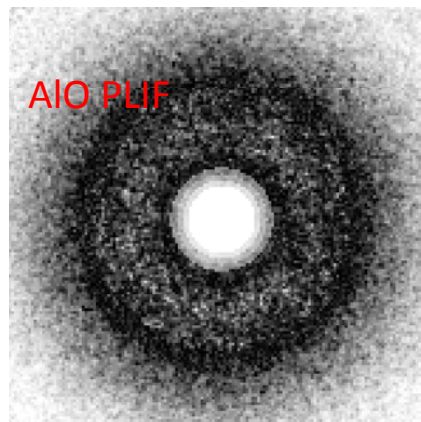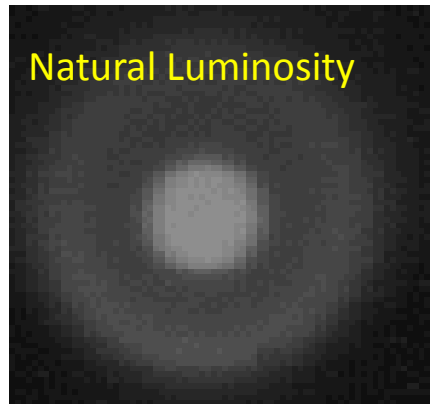
Equilibrium Product Composition and Temperature vs. Input Enthalpy

Stoichiometric Mixture of Al and O_2 at 298 K and 1 atm

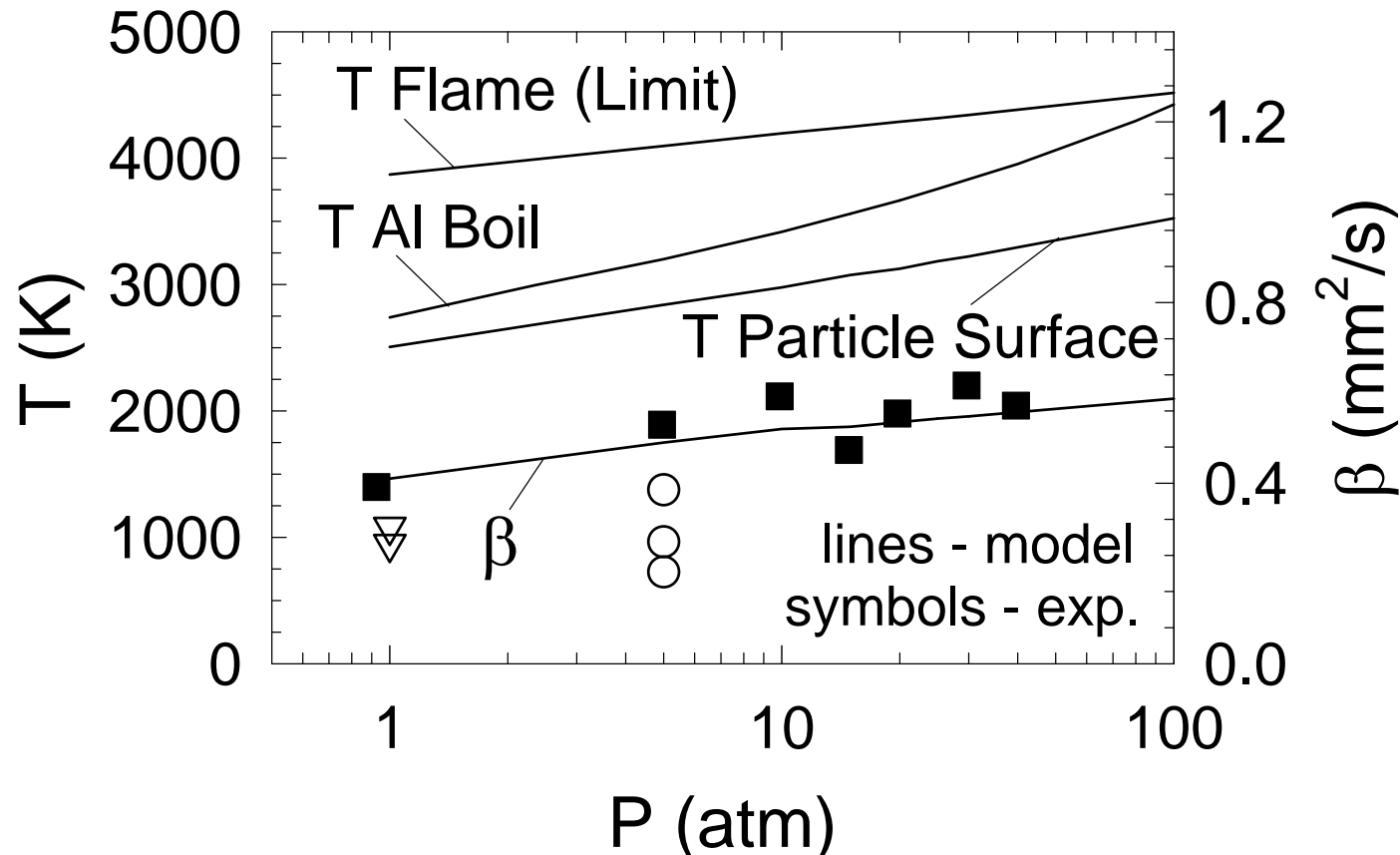Glassman, Combustion, Academic Press, 3rd Edition, 1996
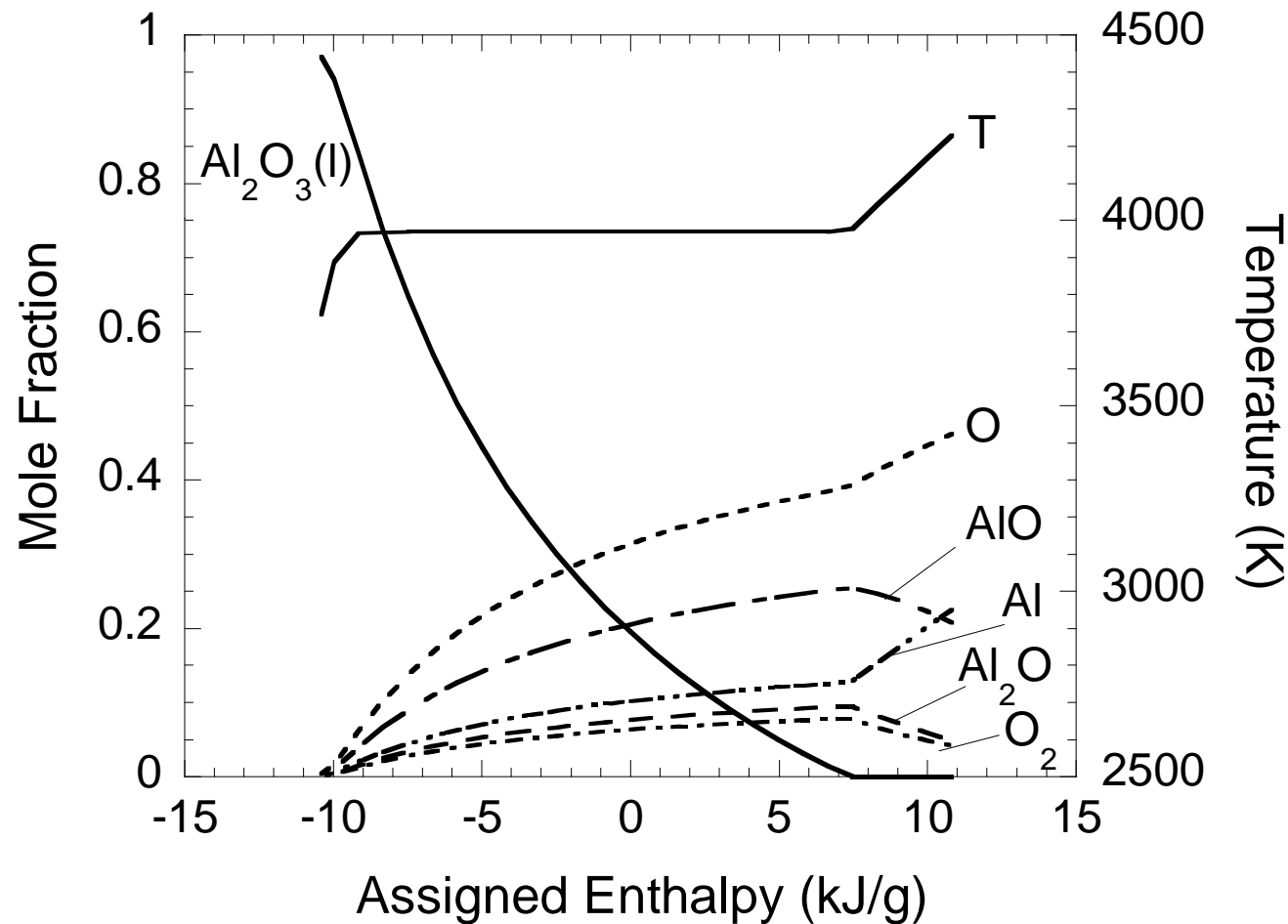
Flame Structure of Micron Aluminum Particle Burning in Air

Bucher, P., *et al. Proc. Combust. Inst.*, 27, 2421, 1998.

Predicted burning rates as a function of pressure for aluminum combustion in 21% O_2 and 79% Ar
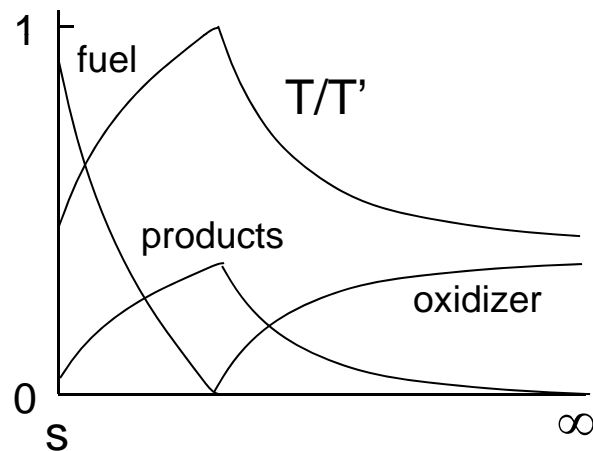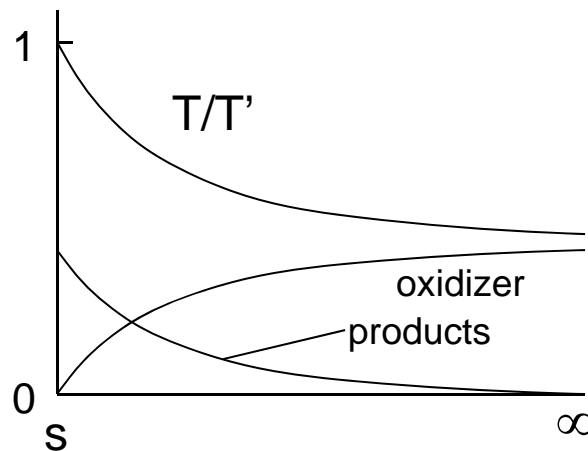
$$d^2 = d_0^2 - \beta t$$

Also shown are the particle surface and maximum flame temperatures
and the vaporization/decomposition temperatures of Al and Al_2O_3
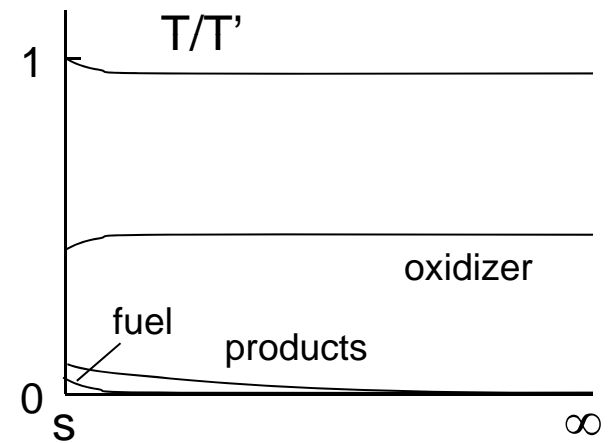
Modes of Particle Combustion

Diffusion-Controlled with Envelope Flame

Diffusion-Controlled without Envelope Flame

Kinetically-Controlled

Diffusion vs Kinetic Control

Diffusion controlled combustion with vaporization or surface reaction

$$t_{b,diff} = \frac{\rho_p d_0^2}{8\rho D \, ln(1+B)} \qquad\qquad t_{b,diff} = \frac{\rho_p d_0^2}{8\rho D \, ln(1+iY_{O,\infty})}$$
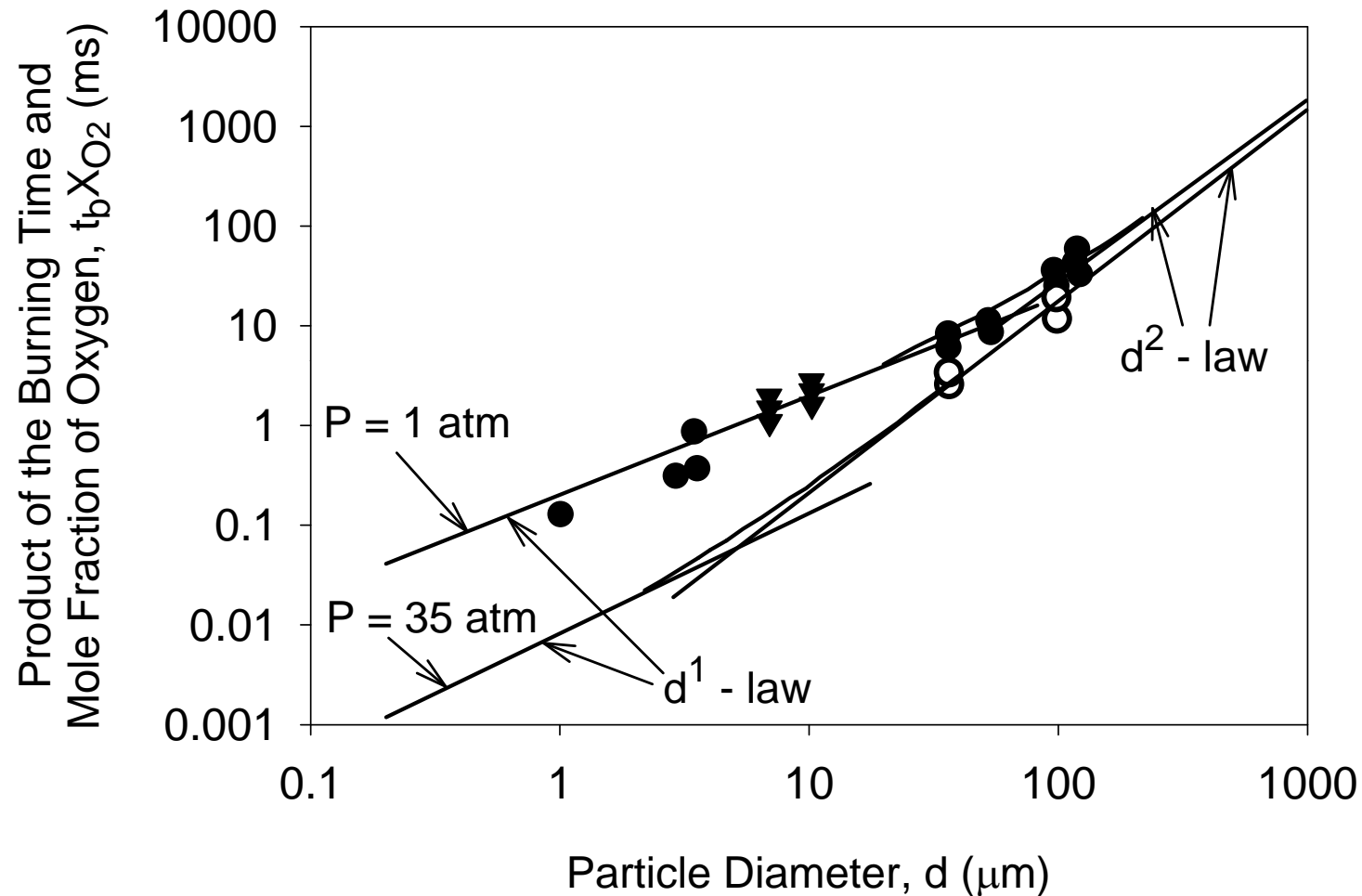
Kinetic controlled surface reaction

$$t_{b,kin} = \frac{\rho_p d_0}{2MW_p kPX_{O,\infty}}$$
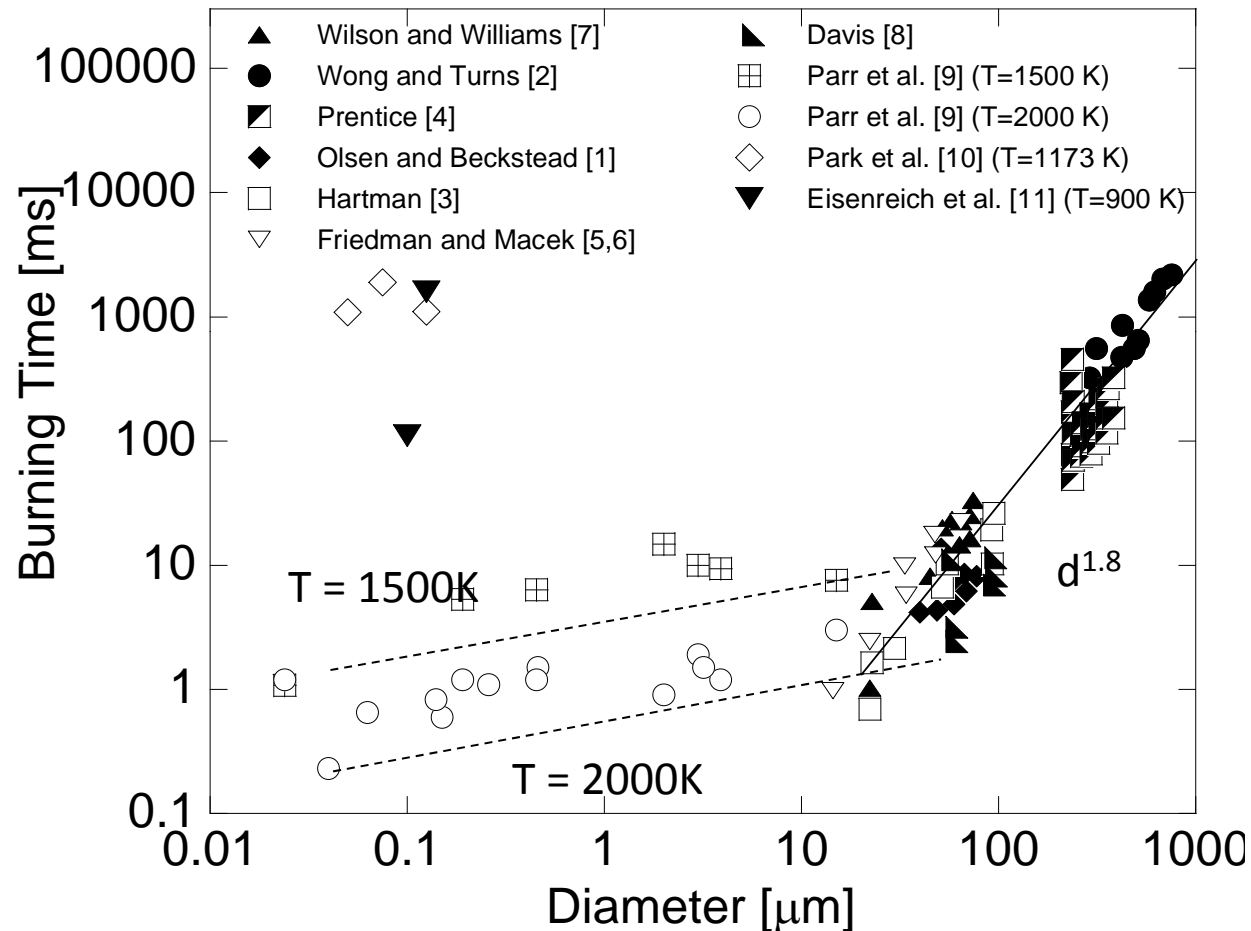
Transition may be defined through a Damköhler number

$$Da = \frac{t_{b,diff}}{t_{b,kin}} = \frac{MW_p kPd_0 X_{O,\infty}}{4\rho D \, ln(1+iY_{O,\infty})}$$

Burning Times of Boron Particles

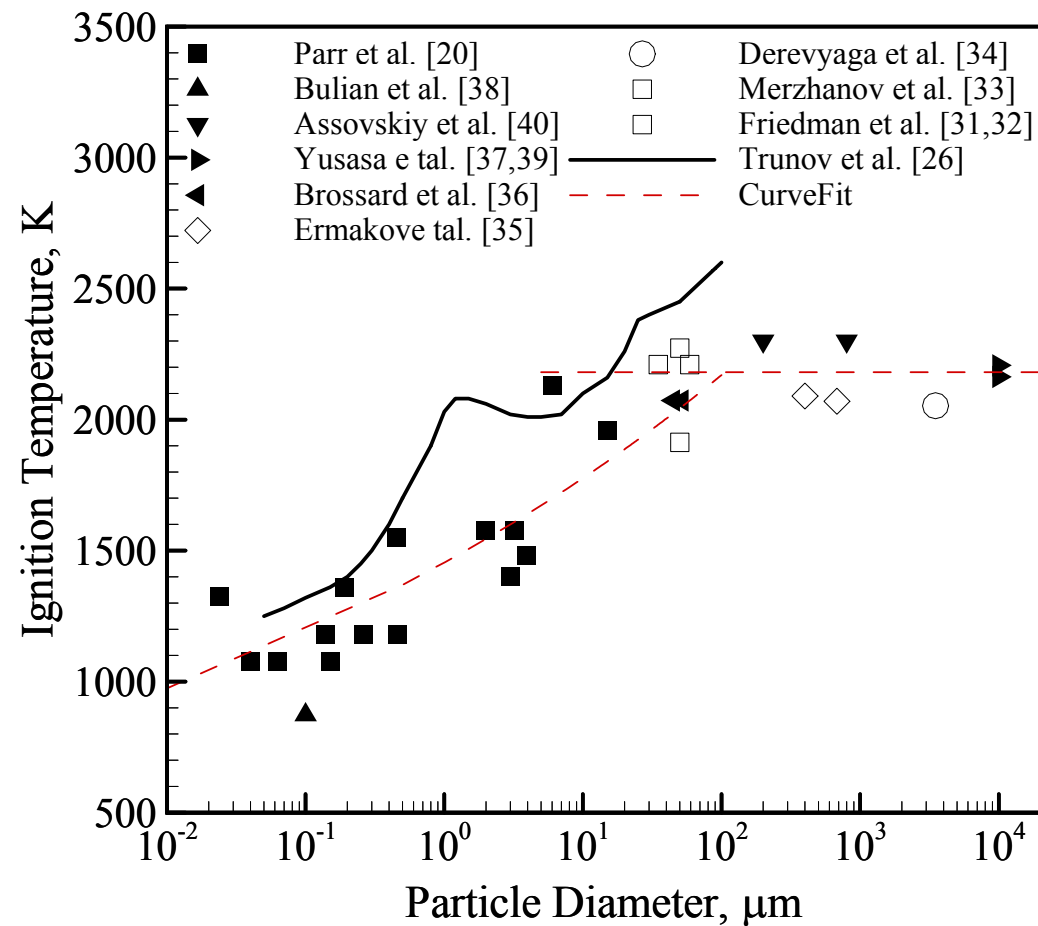Li, S.C. and Williams, F.A. Proc. Combust. Inst. 23, 1147-1154, 1991.

Effect of Particle Diameter on Al Burning Time

T. Bazyn, H. Krier, and N. Glumac, *Proc Combust. Inst*. 31 (2007) 2021 & *Combust. Flame* 145 (2006) 703.
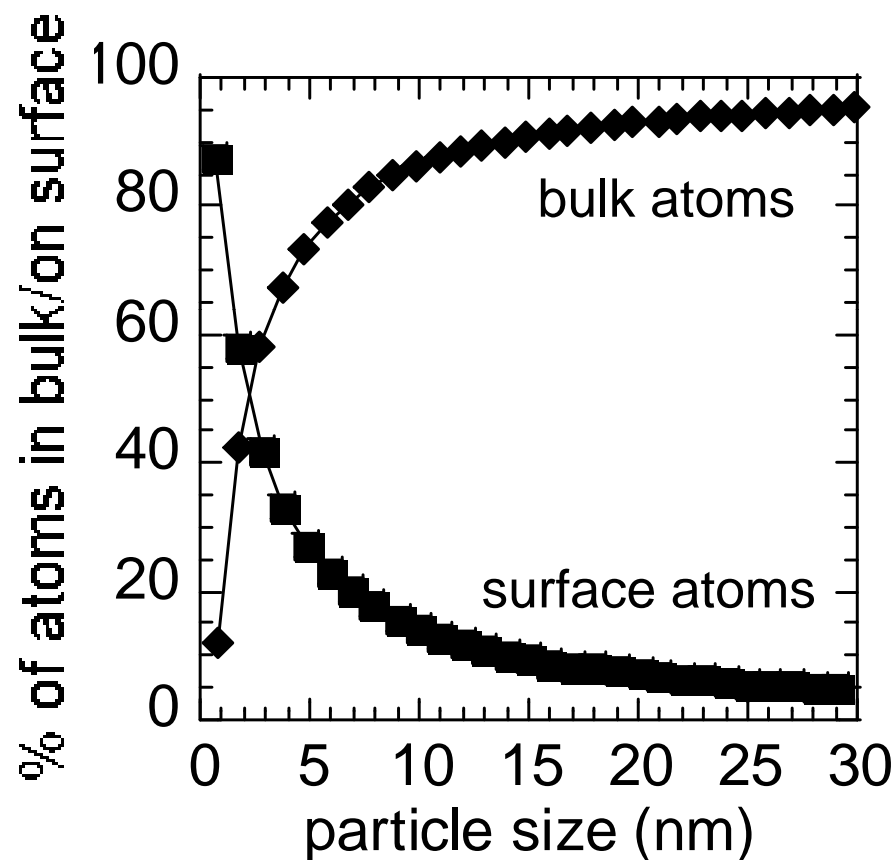
Y.L. Shoshin and E.L. Dreizin, *Combust. Flame* 145 (2006) 714.

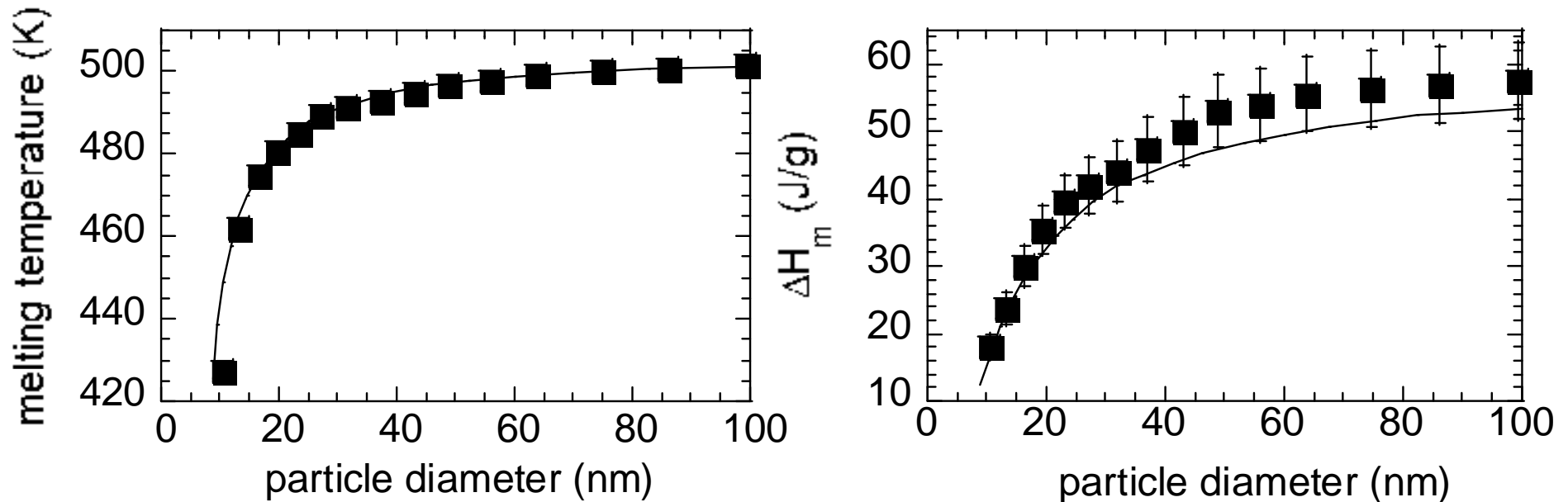# Effect of Particle Diameter on Al Ignition Temperature

Nanoparticle Combustion

Surface to Bulk Atom Ratio for Spherical Iron Crystals

K.J. Klabunde, J. Stark, O. Koper, C. Mohs, D.G. Park, S. Decker, Y. Jiang, I. Lagadic and D.J. Zhang, *J. Phys. Chem*. 100, (1996) 12142-12153.

Melting Point and Normalized Heat of Fusion for Tin Nanoparticles

S.L. Lai, J.Y. Guo, V. Petrova, G. Ramanath, and L.H. Allen, *Phys. Rev. Lett*. 77 (1996) 99-102.

For aluminum particles:
Alavi, S. and Thompson, D.L., *JPC A* 110, 1518, 2006.
Puri, P. and Yang, V., *JPC C* 110, 11776, 2007. Also AIAA 2008-938 and AIAA 2007-1429.

Other Features of Nanoparticles

- Increased specific surface area
- Increased reactivity
- Increased catalytic activity
- Lower melting temperatures
- Lower sintering temperatures
- Superparamagnetic behavior
- Superplasticity

Energy Content as a Function of Particle Diameter
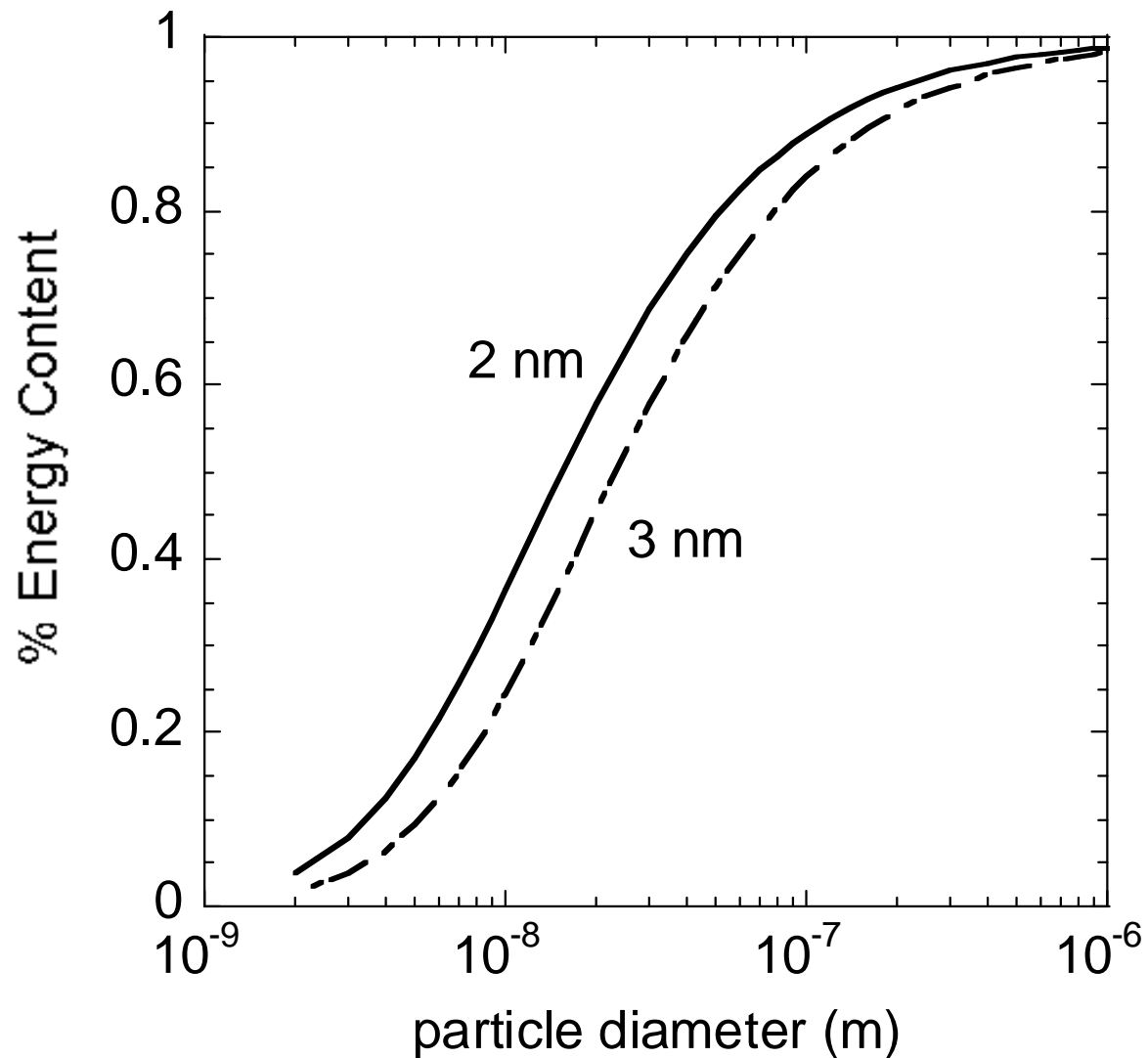
A Brief History of Nanoenergetic Materials

- Synthesis of Energetic Nanoparticles
  - Nanoscale particles readily available
  - Simple substitution for micron sized materials
- Assembly of Energetic Materials
  - Various assembly and additive manufacturing processes: self assembly, sol-gel chemistry, ink-jetting, vapor deposition processes, electro and cold spray, arrested reactive milling, supercritical processing
  - Multilayer foils, core shell structures, reactive nanowires, directly assembled particles, dense nanocomposite powders produced by arrested reactive milling, nanoporous particles and substrates, clusters
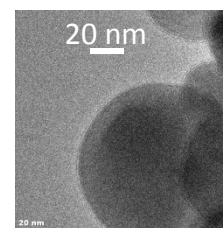
nAl

40 nm
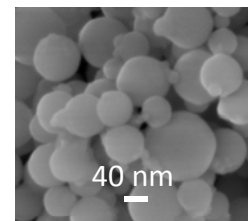
Nanotechnology

RESS nRDX

100nm
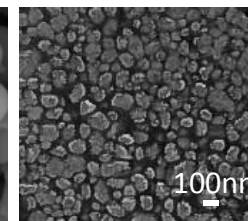
A. Cortopassi, T. Wawiernia, J. T. Essel, P. Ferrara, K. K. Kuo, and R. M. Doherty, 8-ISICP, 2009

L-ALEX

20 nm

T. Sippel and S.F. Son, TEM of palmitic acid coated ALEX

Fe_0-AOT

10 nm
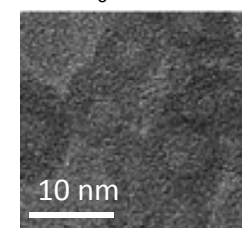
C.E. Bunker and J.J. Karnes, JACS 126, 10852, 2004

Al-$C_{13}F_{27}$COOH

100nm

R.J. Jouet, A.D. Warren, D.M. Rosenberg, V.J. Bellitto, K. Park, and M.R. Zachariah, Chem. Mater. 17 (2005) 2987-2996.

CL-20/NC Cryogel

200nm

T. B. Brill, B. C. Tappan and J. Li (2003). MRS Proceedings,800, AA2.1doi:10.1557/PROC800AA2.1

Nanometer Particles

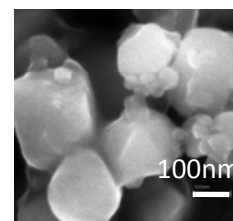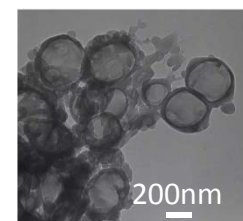Another length scale of importance to the combustion of small particles is the mean free path in the surrounding gas-phase. A comparison of this length scale to the particle diameter defines whether continuum conditions exist (i.e., the particle may be distinguished separately from the gas molecules). The key dimensionless group that defines the nature of the surrounding gas to the particle is the Knudsen number,

$$Kn = \frac{2\lambda}{d_p}$$

where λ is the mean free path of the gas-phase

$$\lambda = \frac{1}{\sqrt{2}\pi\sigma^2 N}$$

where σ is the molecular diameter of the molecule and N is the gas concentration (number density)

$$\lambda = \frac{2\mu}{P\left(\frac{8MW}{\pi RT}\right)^{1/2}}$$

where μ is the gas viscosity and MW is the molecular weight of the gas. At atmospheric pressure, particles of 100 nm and smaller are characterized by Kn numbers greater than unity for the entire temperature range from room to combustion flame temperatures, indicating that they can no longer be considered as macroscopic particles in a continuum gas.

Nanometer Particles

For Kn numbers of the order of 1, expressions used to model heat and mass transfer in the continuum limit are no longer applicable.

- appearance of a discontinuity in temperature, velocity, and concentration profiles at the gas-surface interface, often referred to as slip or jump.
- magnitude of slip depends on the efficiency of exchange of energy and momentum between the gas and surface.
- efficiency is quantified in accommodation coefficients α of a gas-surface interface. For example, the thermal accommodation coefficient α_T is defined as:

$$\alpha_T(T_s, T_g) = \frac{T_f - T_g}{T_s - T_g}$$

where T_s is the surface temperature, T_g is the temperature of the gas incident on the surface, and T_f is the temperature of the gas after scattering from the surface. The value of α_T depends on the gas and surface temperatures in addition to the nature of the gas and surface. The convective heat transfer coefficient h can then be related to α_T in the transition regime by

$$h = \frac{\alpha_T}{8} \frac{Pc}{T_g} \frac{\gamma + 1}{\gamma - 1}$$

where c is the mean speed of the gas.

Nanometer Particles

- Experimental measurements of thermal accommodation coefficients suggest that α_T values at elevated temperatures for some systems are of the order of 0.1, and some may be much lower.
- As the Knudsen number increases, heat and mass transfer are reduced significantly by non-continuum effects.
- In the kinetic limit, transport of mass (and heat for Le ~ 1) is rapid, and concentration and temperature profiles are relatively flat.
- However, for isolated burning of nanoparticles, particle temperatures can rise hundreds of degrees above ambient during combustion at elevated pressures, while for lower pressures the temperature overshoot (as well as the combustion rate) is reduced.
- These observations suggest that although $Kn > 1$ for some nanoparticle systems, the combustion has not reached the kinetic limit due to inhibited transport in the non-continuum regime. Such particles can be considered to be burning in a "transition" regime between the diffusion and kinetic limit, in which neither the d^2 nor d burning rules apply.

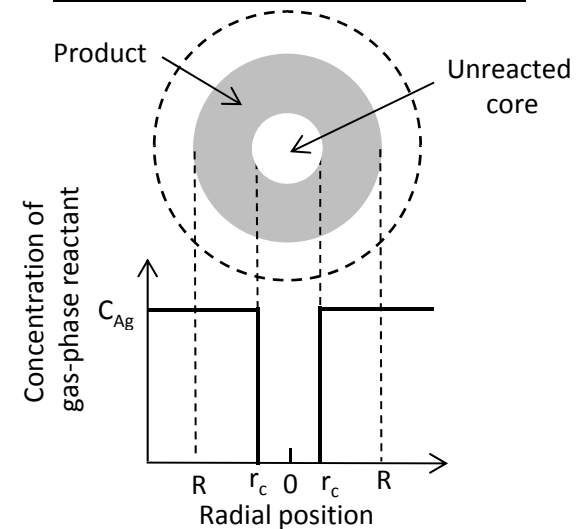# Shrinking Core Model for Spherical Particles of Unchanging Size
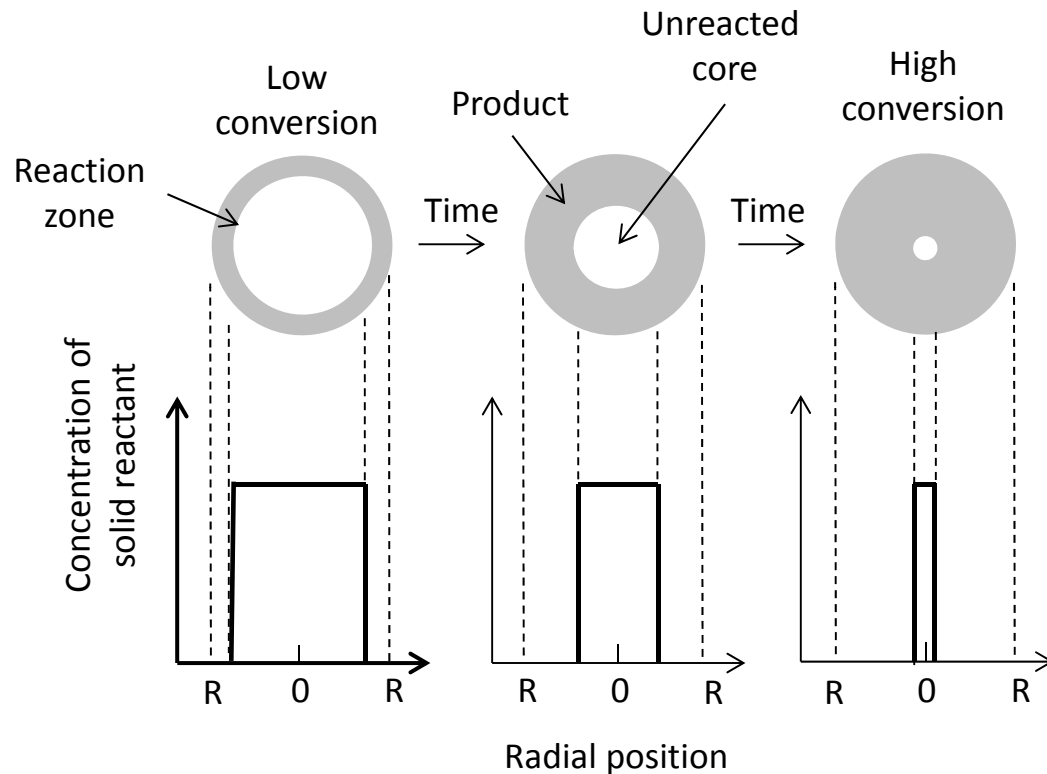
Diffusion through Product Layer Controls

See for example, Levenspiel, O., Chemical Reaction Engineering, Third Edition, J. Wiley and Sons, 1999
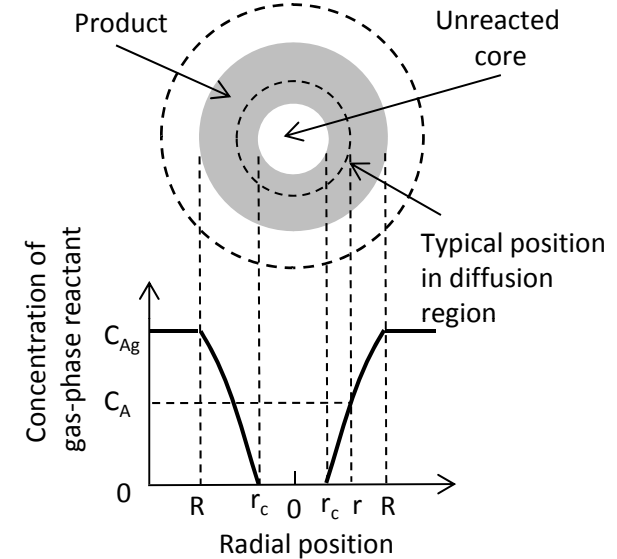
Chemical Reaction Controls

Shrinking Core Model for Spherical Particles of Unchanging Size

Diffusion through Product Layer Controls

$$\tau = \frac{\rho_p R^2}{6bDC_{Ag}}$$

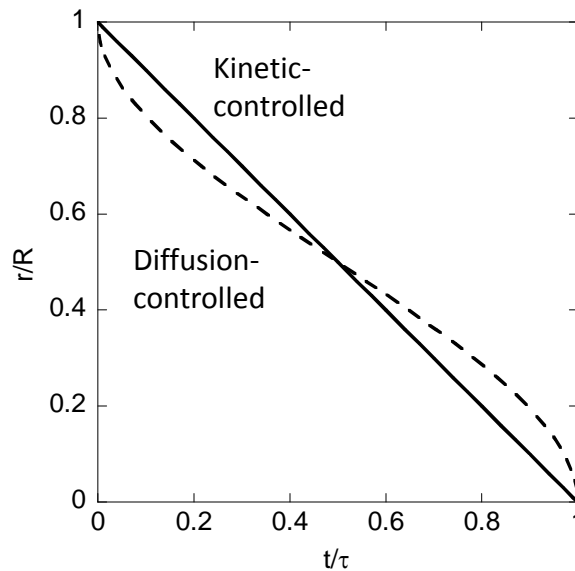$$\frac{t}{\tau} = 1 - 3\left(\frac{r}{R}\right)^2 + 2\left(\frac{r}{R}\right)^3$$

$$\frac{t}{\tau} = 1 - 3(1-X)^{2/3} + 2(1-X)$$

Chemical Reaction Controls

$$\tau = \frac{\rho_p R}{bkC_{Ag}}$$

$$\frac{t}{\tau} = 1 - \frac{r}{R}$$

$$\frac{t}{\tau} = 1 - (1-X)^{1/3}$$

Radius vs. Time

Kinetic-controlled

Diffusion-controlled

(r/R vs. t/τ)

Conversion vs. Time

Kinetic-controlled

Diffusion-controlled

(1-X vs. t/τ)
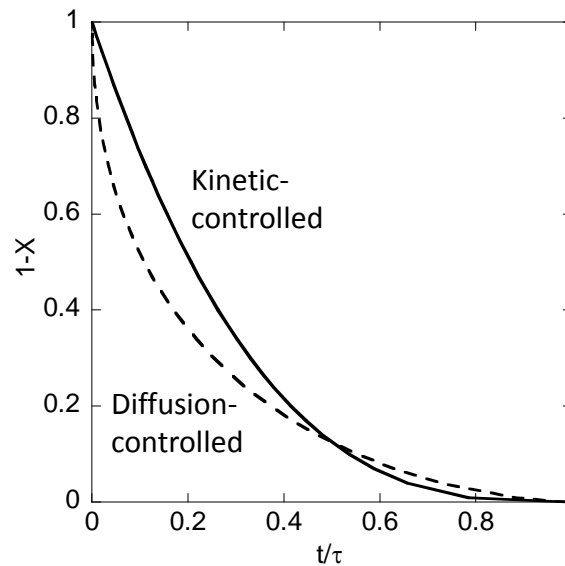
Rate of Change of Conversion vs. Conversion

Diffusion-controlled

Kinetic-controlled

(d(1-X)/d(t/τ) vs. X)

See for example, Levenspiel, O.,Chemical Reaction Engineering, Third Edition, J. Wiley and Sons, 1999
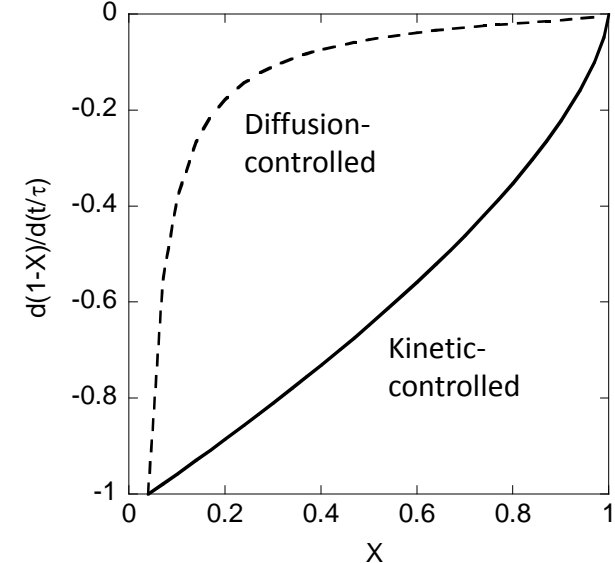
Schematic of Melt-Dispersion Mechanism of Combustion of Nano Aluminum Particles at High Heating Rate (>10^6 K/s)

Aluminum core covered by initial alumina shell
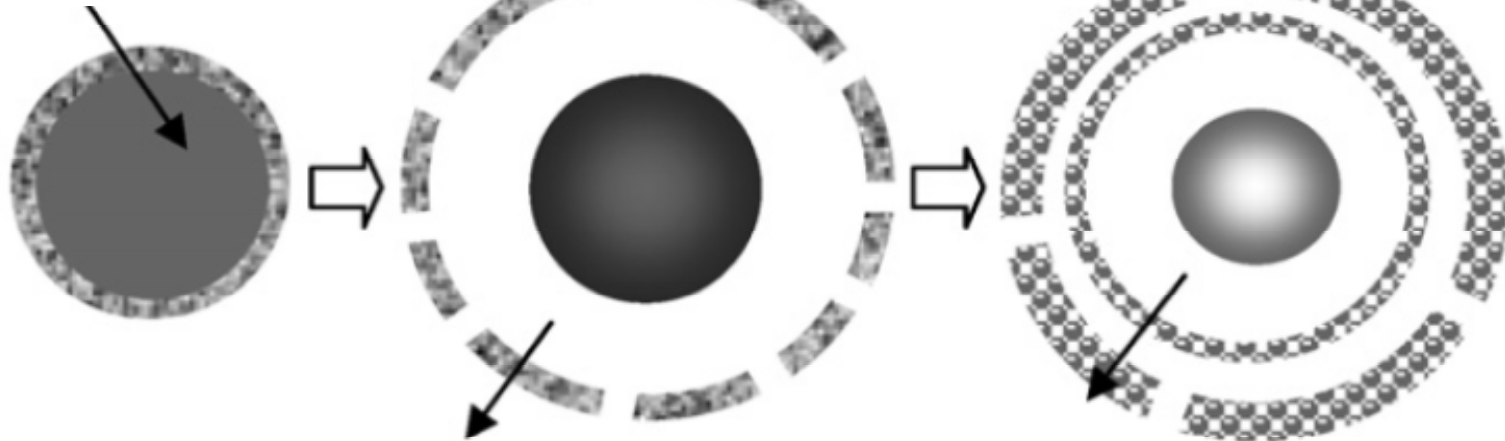
Fast melting of Al leads to spallation of the alumina shell

Unloading wave propagates to the center of Al molten core and generates tensile pressure which disperses small Al custers

Molecular dynamic simulation snapshots of the central slice of a 26 nm Al particle covered with an oxide shell 3 nm thick

- Oxidation starts after core & shell heated to 1100 K
- As oxidation begins, due to expansion of molten core, the size grows
- Oxidation dynamics starts with the Al-NP at the core shell interface when molten Al reacts with alumina shell taking O to form Al rich Al_xO_y clusters, which generates heat
- Shell does not break or shatter, only deforms
- When $T \sim 2900$ K, the alumina shell melts and Al ejections occur from Al-NP into oxygen environment producing oxygen rich Al_xO_y clusters
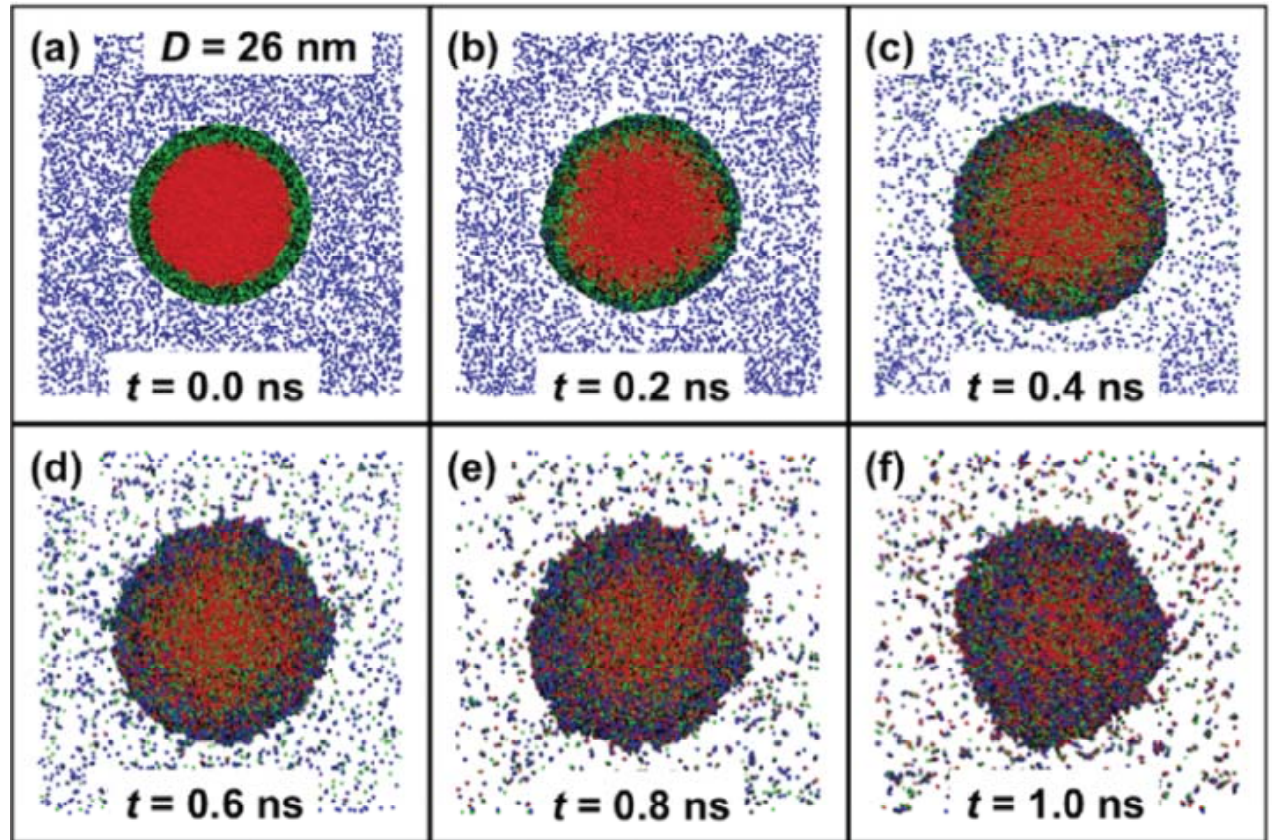
Blue = envirnomental oxygen
Red = core Al atoms
Black = shell Al atoms
Green = shell O atoms

Li et al., J. Applied Phys. 114, 13, 134312, 2013

Thermal Gravimetric Analysis of Nanoaluminum with CO_2
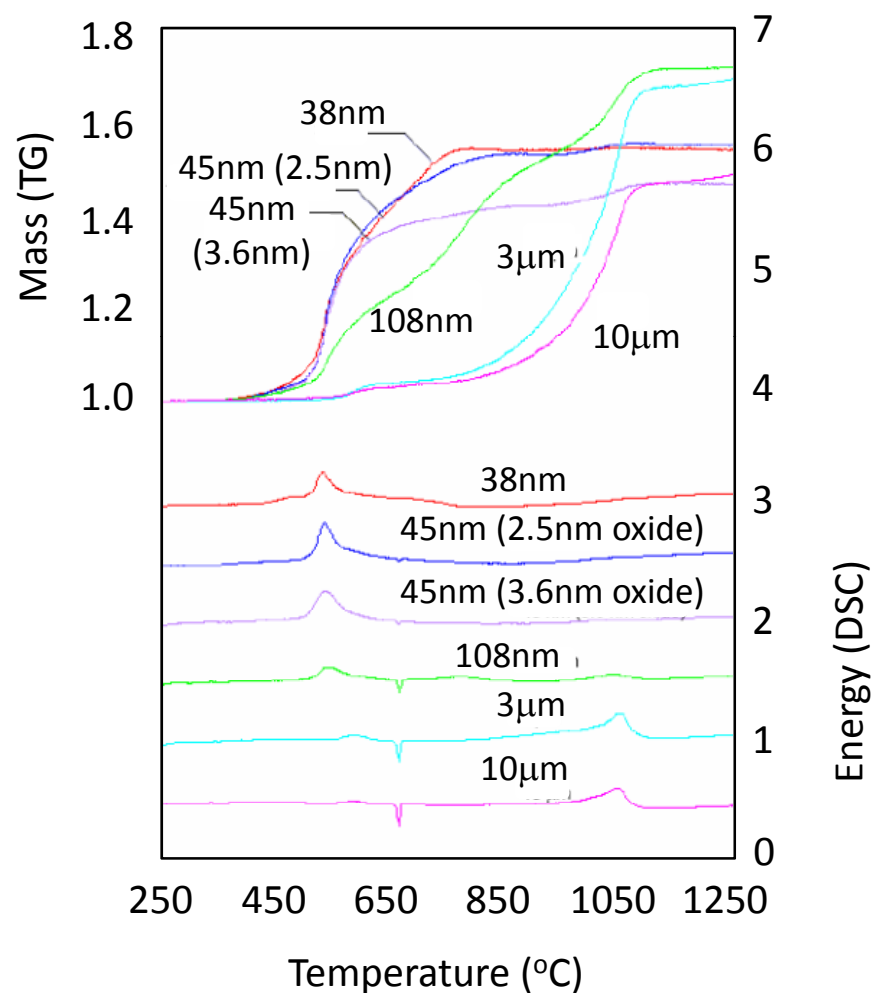
K. Brandstadt, D. L. Frost, and J. A. Kozinski, in Advancements in Energetic Materials and Chemical Propulsion, ed. K.K. Kuo and J. de Dios Rivera, Begall House, 2007.
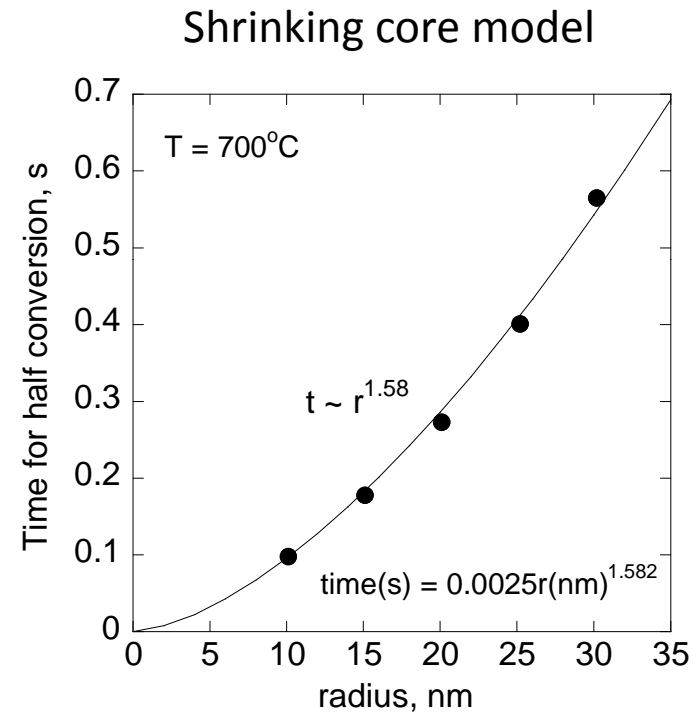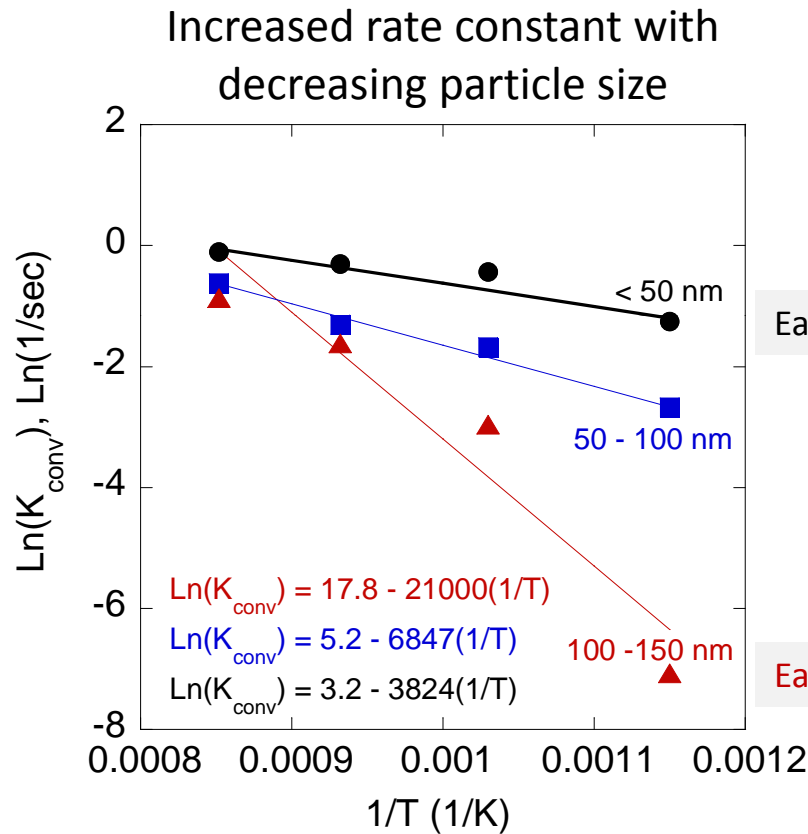Il'in AP, Gromov AA, and Yablunovskii GV (2001) Combustion, explosion, and shock waves, 37 n.4: 418-422.

Polymorphic Phase Transformations in Al$_2$O$_3$ Layer
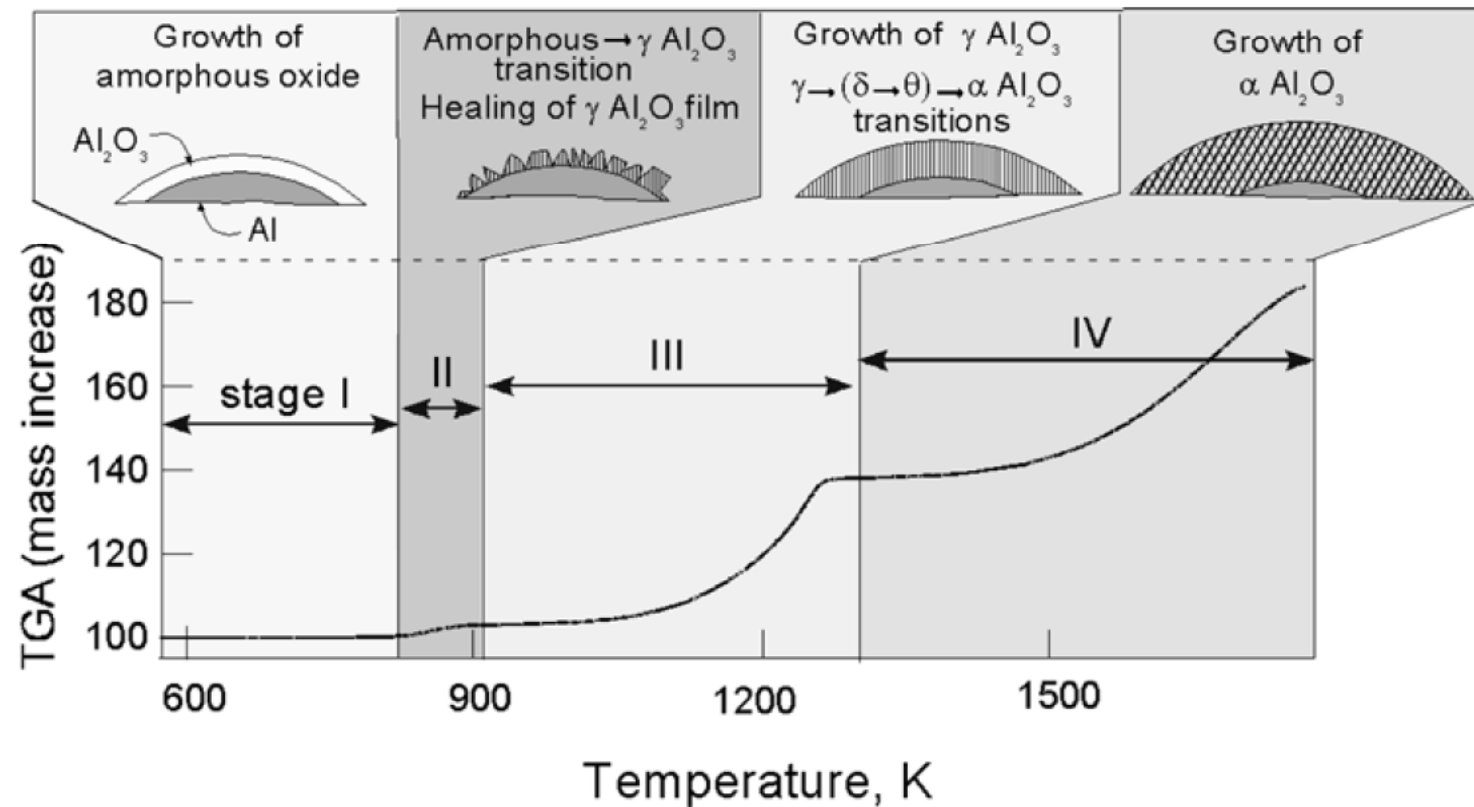
M. A. Trunov, M. Schoenitzand E. L. Dreizin, *Combustion Theory and Modelling*, 10, 2006, 603–623

Aluminum Nanoparticle Oxidation with Single Particle Mass Spectrometry

Increased rate constant with decreasing particle size

Shrinking core model

Ea ~ 32kJ/mol

Ea ~ 95kJ/mol

$Ln(K_{conv}) = 17.8 - 21000(1/T)$

$Ln(K_{conv}) = 5.2 - 6847(1/T)$

$Ln(K_{conv}) = 3.2 - 3824(1/T)$

< 50 nm

50 - 100 nm

100 - 150 nm

T = 700°C

$t \sim r^{1.58}$

$time(s) = 0.0025r(nm)^{1.582}$

Effective diffusion coefficient (D_e) of oxygen in ash layer = $10^{-9} \sim 10^{-8}$ cm^2/s for < 50 nm particles
At temperatures above ~ 1000°C, hollow particles formed.

K. Park, D. Lee,† A. Rai, D. Mukherjee, and M. R. Zachariah, J. Phys. Chem. B 2005, 109, 7290-7299
A. RAI, K. PARK, L. ZHOU and M. R. ZACHARIAH, Combustion Theory and Modelling, Vol. 10, No. 5, October 2006, 843–859

Combustion of Aluminum Particles in Energetic Materials

Combustion of Aluminum Particles in Energetic Materials

- Aluminum is used as an ingredient in solid propellants because of its high energy density, high heat release during oxidation, low cost, and relative safety

- Because most unaluminized propellants are already fuel rich, it might seem counterproductive to add more fuel (Al)

- However oxidation reduces the oxidizer vapors (H_2O and CO_2) to H_2 and CO, better propulsive fluids

- This in combination with a large increase in temperature, results in an increase in I_{sp} of around 10% and a net gain in propellant mass fraction in the motor of typically 15%

- Aluminum in even the modest amounts suppresses combustion instability problems common in motor development programs

- There are also problems with use of aluminum, such as smoky, luminous exhaust trails, two-phase flow, and slag accumulation

Combustion of Aluminized Solid Propellants

- Aluminum does not turn into vapor at the propellant surface like other primary ingredients (BP$_{Al}$ = 2467°C, usually propellant T$_s$ ~ 600°C, which is ~ 60 deg below the 660°C MP of Al; ρ_{Al} = 2.7 g/cm^3 which is ~ 1.38 times that of AP and 3 times that of HC binders)

- Its reaction or ignition on the surface is inhibited by the refractory oxide coatings on the particle surfaces (MP$_{Al2O3}$=2072°C; Al$_2$O$_3$ constitutes about 0.5% of the particle mass for 25 μm particles)

- The particles tend to adhere to the surface in binder melts, leading to locally higher concentrations

- At temperatures between the Al and Al$_2$O$_3$ melting points, leaking of Al from the oxide coating can lead to sintering in assemblages of particles into *sintered accumulates*. The leakage can be so great that the Al engulfs the entire assemblage to form *spherical agglomerates*.

Combustion of Aluminized Solid Propellants

- When aluminum particles are heated the oxide structure changes, and the aluminum expands. The coefficient of expansion of the oxide skin is less so that it must be stressed. At the melting point of Al, it expands in volume about 6%, thereby stressing the oxide skin further and potentially causing cracks.

- The concentrations of typically 20 μm particles can lead to coalescence into large droplets (e.g., typically 200 μm containing 10^3 original particles).

- Large droplets leave the surface and burn in the gas flow field (typically with H_2O and CO_2), whereas any original particles that leave the surface individually burn up within 1 to 2 mm of the surface (with a corresponding greater effect on the propellant burning)

- In small motors, large droplets may not burn up completely, reducing I_{sp}

Aluminum Particle Combustion

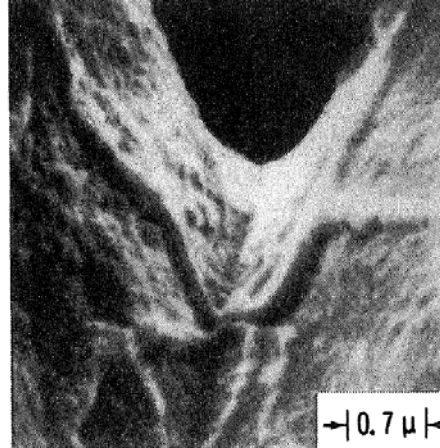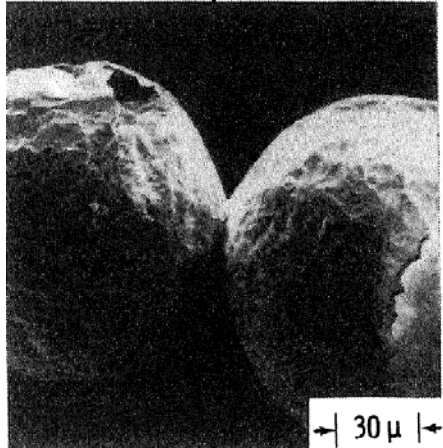Image from a small sample of the space shuttle propellant
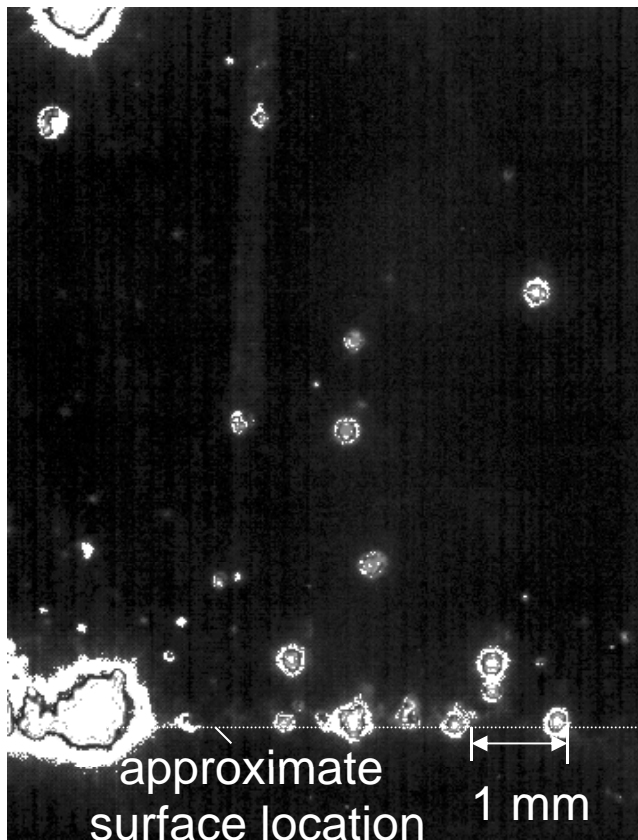
Magnified video image from a small sample of a nitramine propellant

approximate surface location

1 mm

streamer

oxide cap

Al_2O_3

Al agglomerate

200μm
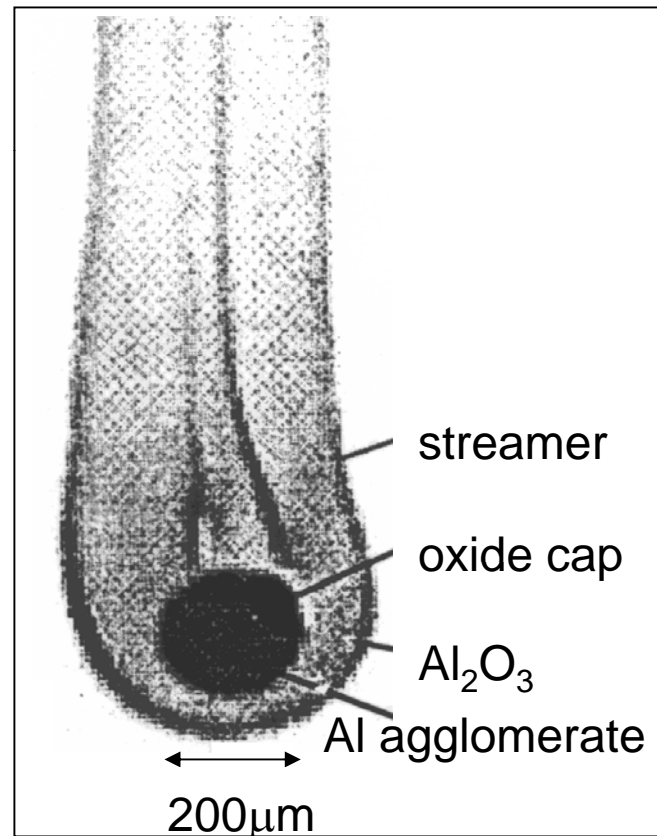
flow direction

Accumulation and Agglomeration

Oxide skins on particles dropped on 1400°C plate showing crack pattern and bridging between particles.

Sintered accumulate, quenched in transition to an agglomerate. Note spherical structures where coalescence of liquid Al has started.
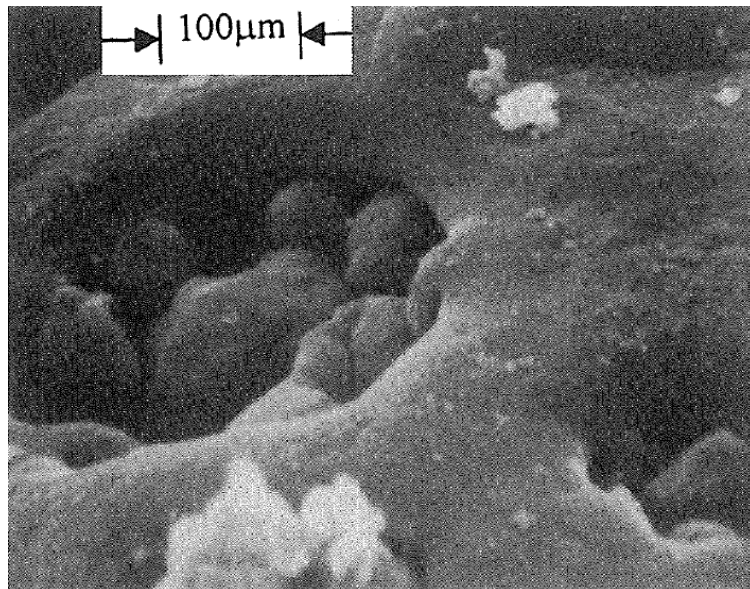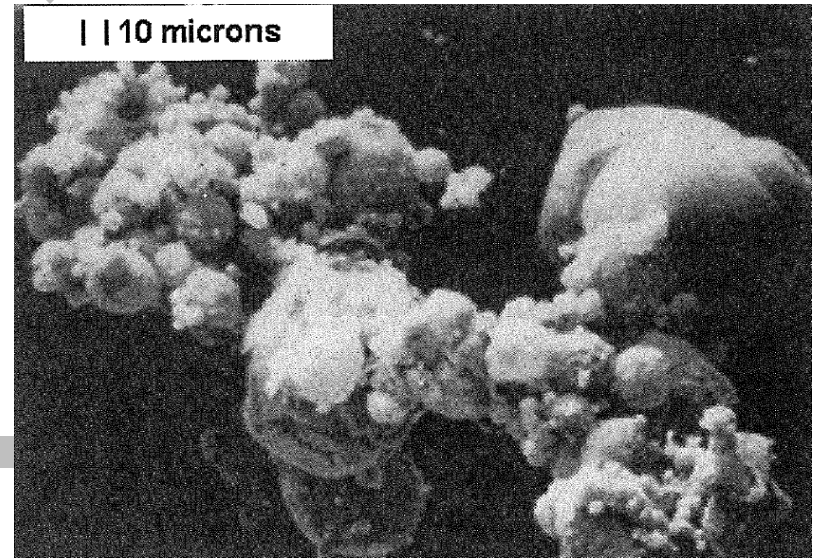

Agglomerate quenched before complete transition to a molten droplet. Al surface tension had drawn the accumulate into a sphere, but not yet closed the surface. Un-melted oxide shells still visible in openings.

Particle Packing

- The stoichiometry of an AP/binder system dictates that a maximum achievable content of AP be used with required propellant processing and mechanical properties
- Typically, a coarse (e.g. 200μm) AP portion is combined with finer particles to fill the spaces left in the coarse particle array
- By careful blending of sizes (e.g., using trimodal particle size), formulations are processed with 86-88% AP by weight (still fuel rich), yielding cured propellants with acceptable mechanical properties
- When Al is added (typically 10-30 μm), a corresponding volume of fine AP is removed
- Thus the Al particles are preconcentrated in pockets of coarse AP packing pattern

Progression of burning front into an aluminized propellant
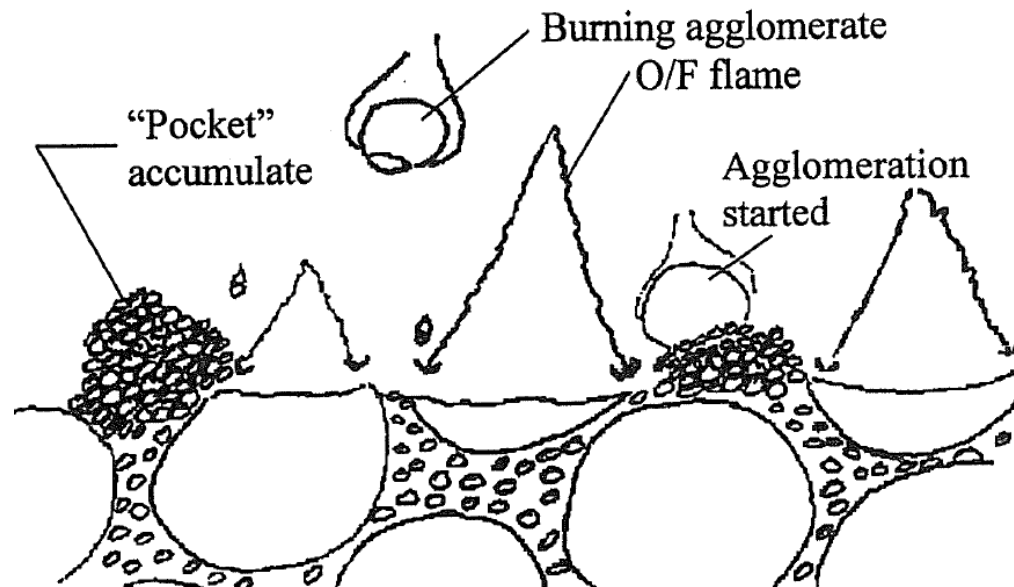
The size distribution of agglomerates on the surface depends on
- The structural features of the Al particle packing
- The surface retention characteristics of the binder (e.g., *particle adhesion in a binder melt layer, retention in a carbonaceous surface structure, direct adhesion to underlying Al particles, centrifugal force in spinning motors*)
- The susceptibility of individual particles to ignition
- Possible connective processes between concentrating particles that lead to group behavior
- Evolution of the underlying structure and hot overlying gas flamelets that lead to detachment-ignition events

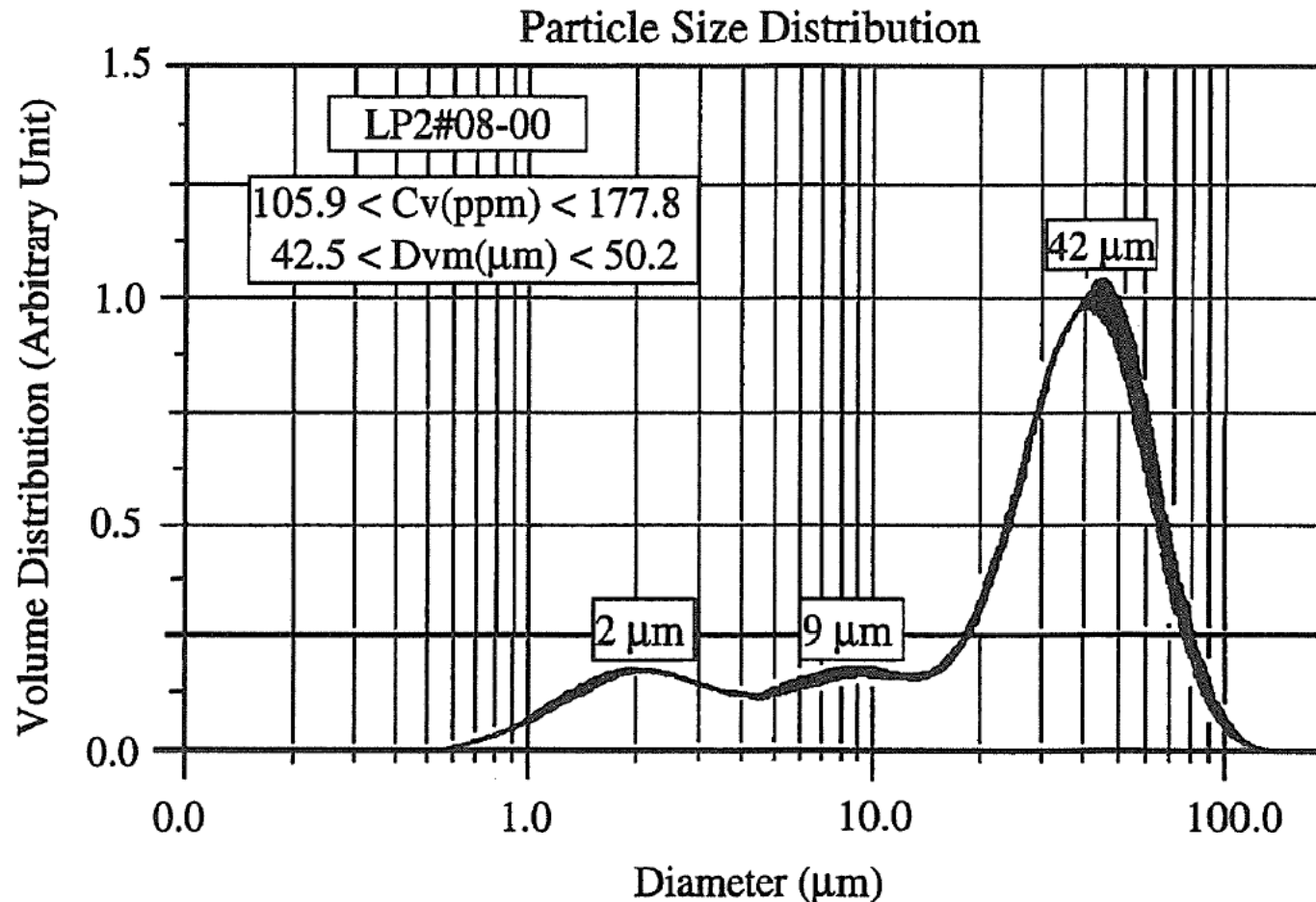# Effect of pressure on mass-average agglomerate size for bimodal propellant

Coarse/fine AP of ratio 8/2

Coarse size 390 μm

Fine size as indicated
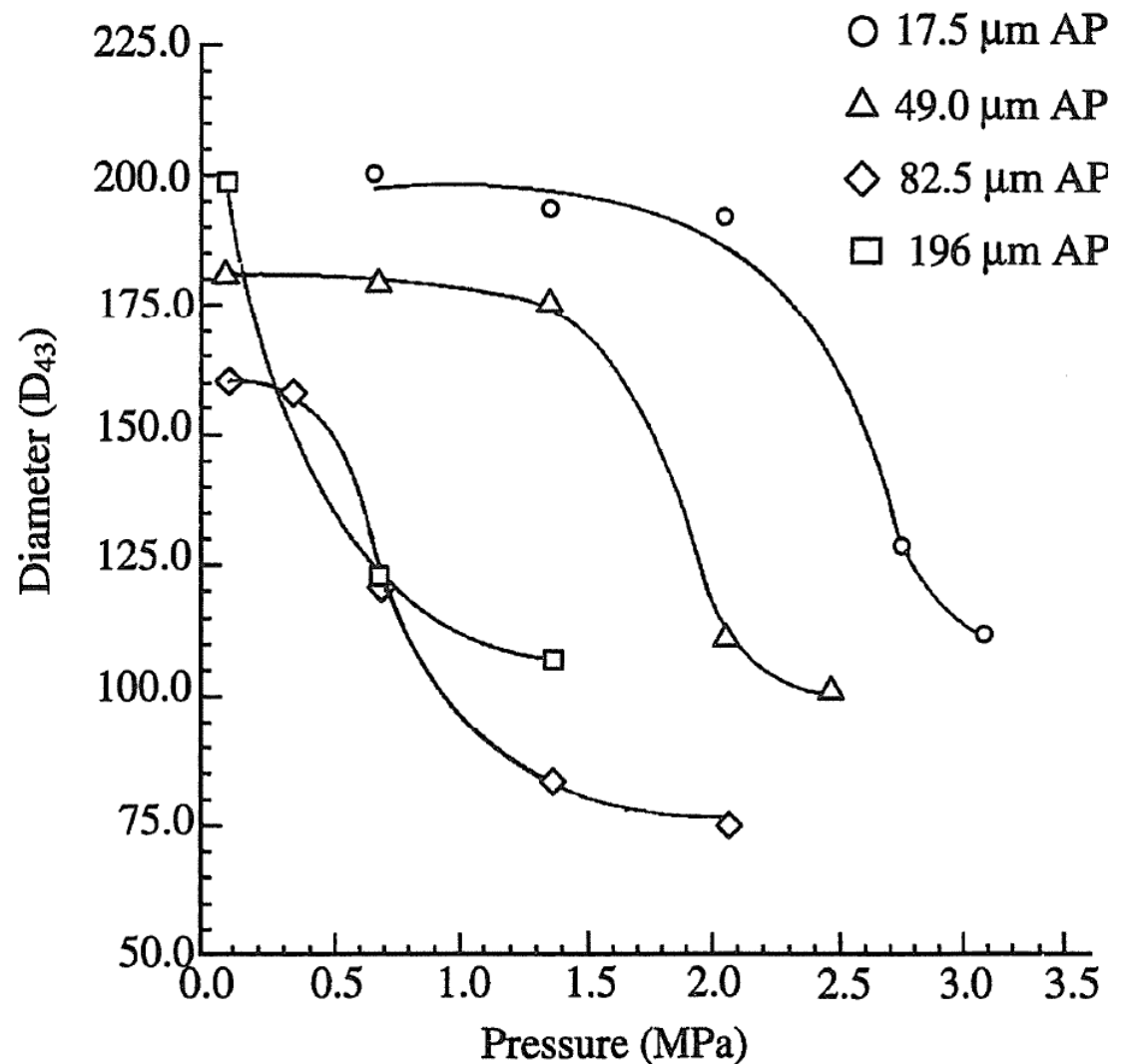
Typical burn-out oxide distribution
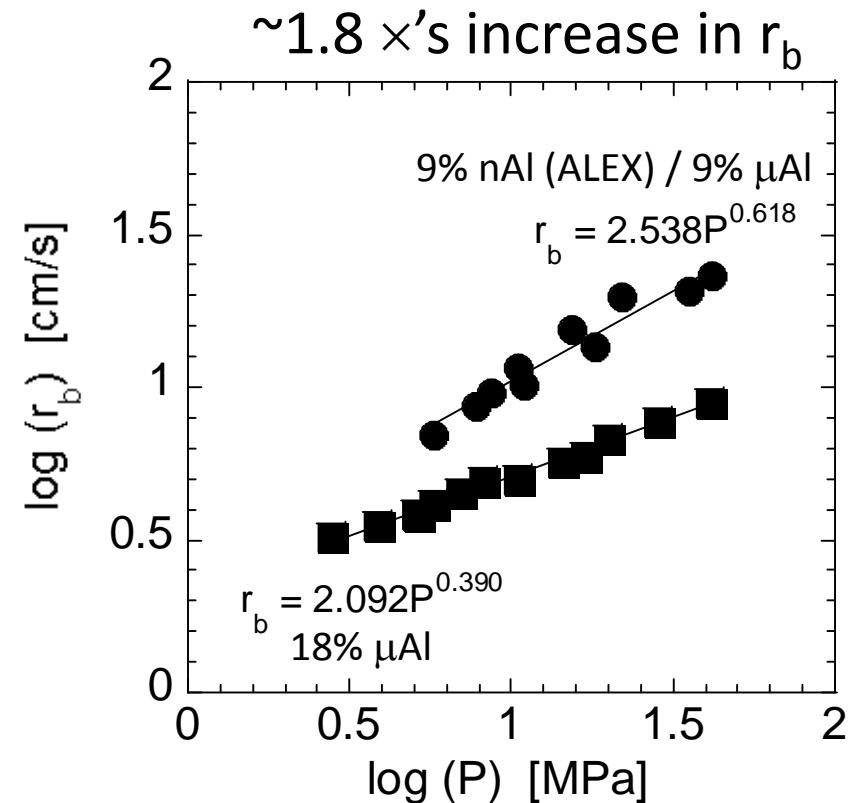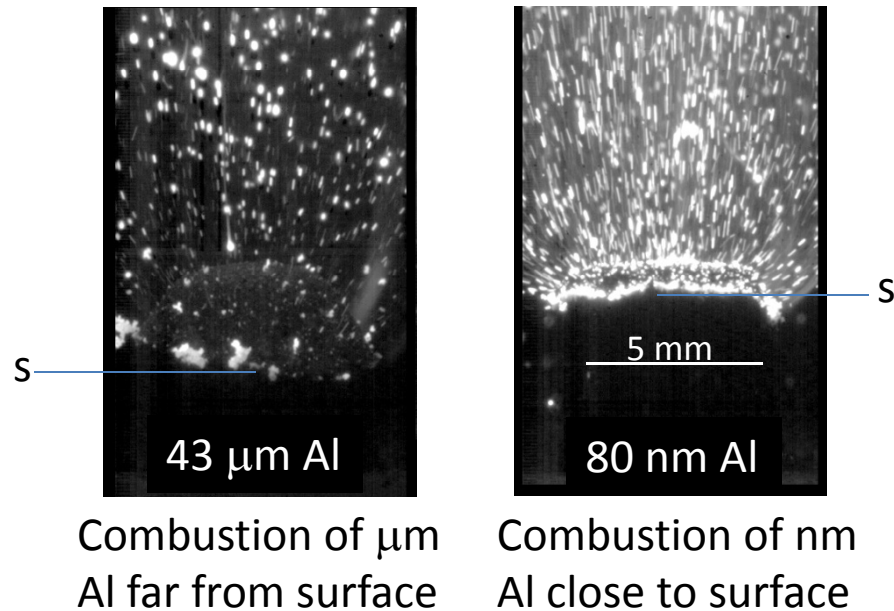

Particle Size Distribution

- Generally, the distribution below 2 μm results from the Al_2O_3 formed in the cloud around the burning particles (smoke), whereas the larger sizes result from Al_2O_3 accumulation on the original Al particles
- From a practical viewpoint, a mean size distribution of 10-25μm is ideal for stabilizing combustor instabilities in the 200-400 Hz range

Factors influencing agglomerates

- Large agglomerates result in large residual oxide droplets
- High aluminum content in the propellant leads to large agglomerates
- Factors that increase burning rate reduce the amount and size of agglomerates
- Ingredient particle size distributions that yield large concentrations of aluminum in the propellant particle packing pattern give large agglomerates
- Use of burning rate suppressants and binders that produce increased melts and carbonaceous residue on the burning surface usually lead to increased agglomeration and agglomerate size
- Modification of the aluminum particles in a way to minimize inter-particle sintering reduces agglomeration (e.g. coatings for aiding ignition, pre-oxidation)
- Cross-flow environments tend to decrease agglomeration

Example of burning propellants with nanometer and micron sized Al particles

43 μm Al

Combustion of μm Al far from surface

s

5 mm

80 nm Al

Combustion of nm Al close to surface

~1.8 ×'s increase in r_b

9% nAl (ALEX) / 9% μAl

$r_b = 2.538P^{0.618}$

$r_b = 2.092P^{0.390}$

18% μAl

log (r_b) [cm/s]

log (P) [MPa]

T. R. Sippel, S. F. Son, L. J. Groven, Aluminum agglomeration reduction in a composite propellant using tailored Al/PTFE particles, Combustion and Flame 161 (2014) 311–321.

Mench, M.M., Yeh, C.L., and Kuo, K.K., "Propellant Burning Rate Enhancement and Thermal Behavior of Ultra-fine Aluminum Powders (ALEX)," in Proc. of the 29th Annual Conference of ICT, 1998, pp. 30-1 – 30-15.
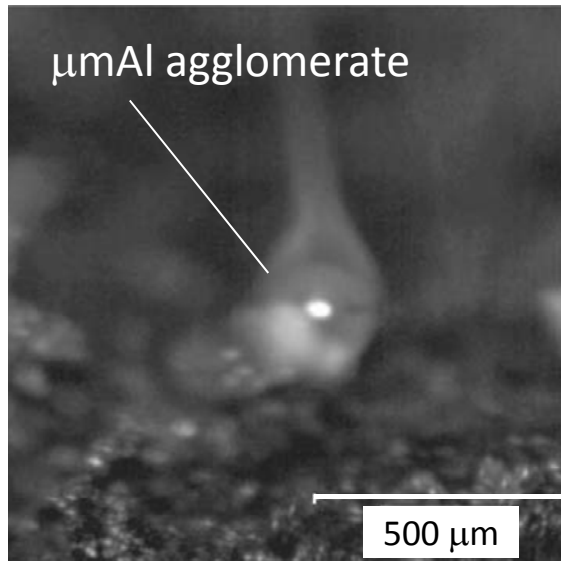
G. V. Ivanov, and F. Tepper, Challenges in Propellants and Combustion 100 Years after Nobel, pp.636-645, (Ed. K. K. Kuo et al., Begell House, 1997).
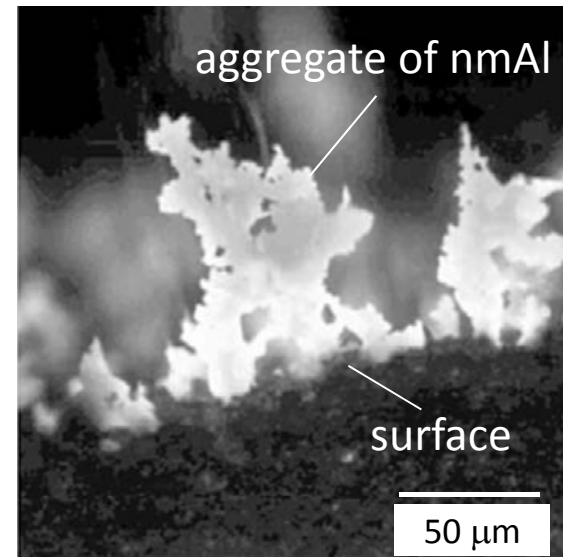
Al Burning Times

Experiment
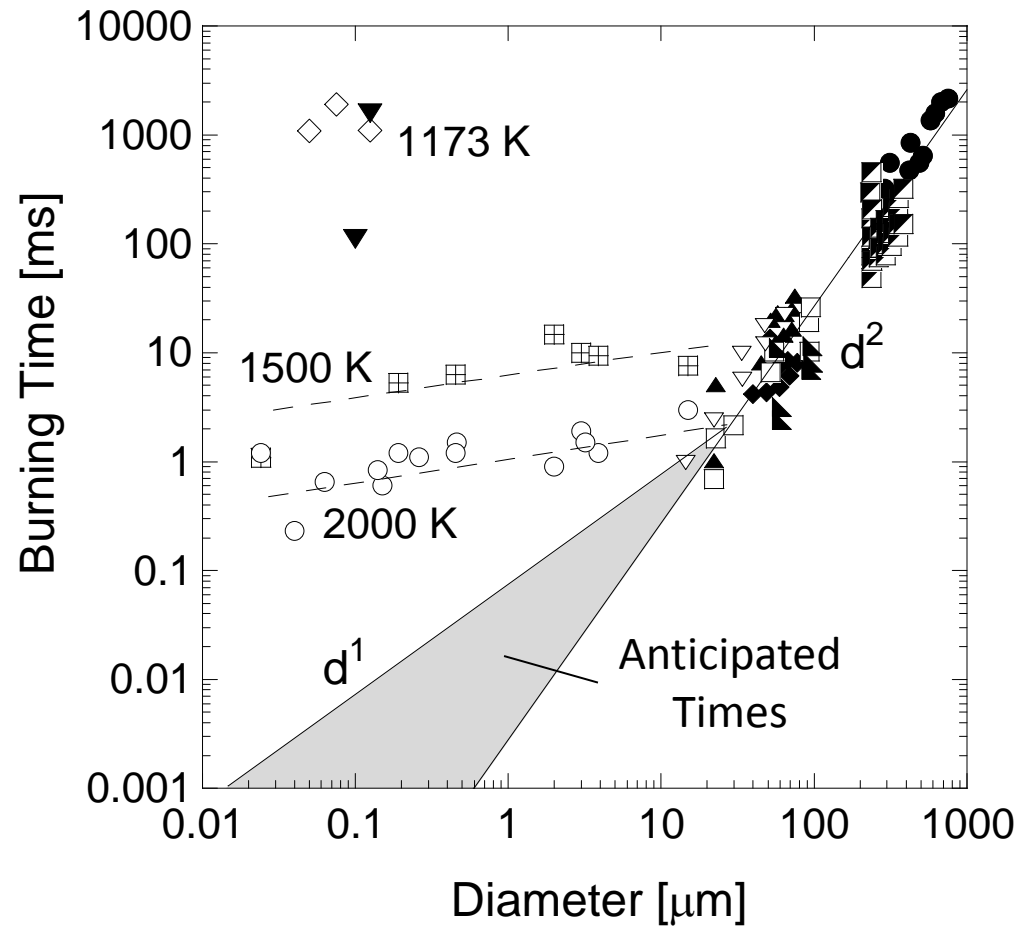
Example of Burning Propellants: the Surface

μmAl agglomerate

500 μm

50 μmAl spherical agglomerate formed by inflammation of an aluminized aggregate

aggregate of nmAl

surface

50 μm

50-250 nmAl emerging from surface as aggregates (pre-agglomerate)

L. T. De Luca, L. Galfetti, F. Severini, L. Meda, G. Marra, A. B. Vorozhtsov, V. S. Sedoi, and V. A. Babuk, Burning of Nano-Aluminized Composite Rocket Propellants, *Combustion, Explosion, and Shock Waves, Vol. 41, No. 6, pp. 680–692, 2005*

Why n ~0.3

- Surface roughness and presence of cracks in oxide layer may alter relationship between d_p and A_s for chemical reactions (Buckmaster and Jackson, Comb Theory Model 17, 335, 2013)
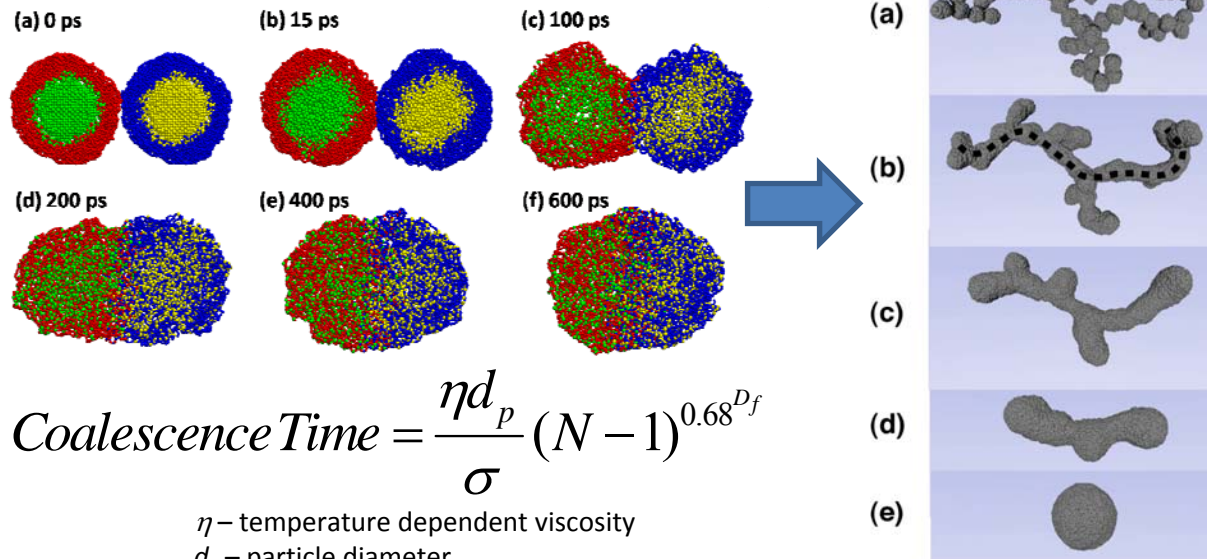
$$A = A_{ref} \left(\frac{d_p}{D_{ref}} \right)^{D_{frac}}$$

$$2 < D_{frac} < 3$$

$$t_b \sim d_p^{3-D_{frac}}$$

- n varies from 1 to 0 as D_{frac} changes from 2 to 3
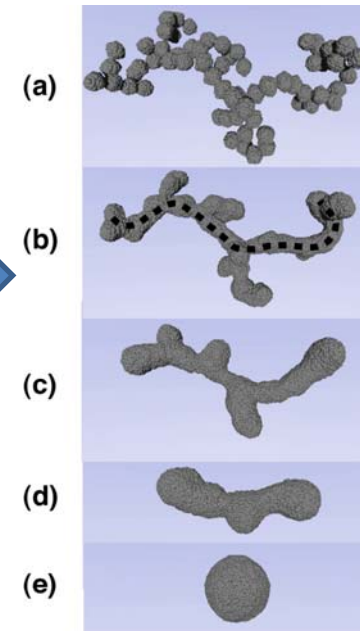- For non-fractal surfaces,
$$t_b \sim d$$

Sintering and reaction times are close that nanostructure is lost before it can be utilized

Sintering of NanoAluminum

(a) 0 ps   (b) 15 ps   (c) 100 ps

(d) 200 ps   (e) 400 ps   (f) 600 ps

$$Coalescence\,Time = \frac{\eta d_p}{\sigma}(N-1)^{0.68^{D_f}}$$

η – temperature dependent viscosity
d_p – particle diameter
σ – surface tension
D_f – aggregate fractal dimension
N - number of primaries

(a)
(b)
(c)
(d)
(e)

P. Chakraborty and M. Zachariah, Combustion and Flame 161 (2014) 1408.

- Sintering time consists of two times: time to heat the particles and the fusion time
- Loss of nanostructure (surface area) in < 20 µs
- Experimental burning times 50-500 µs

What is needed:
- **Approaches that enable smaller length scales, disable sintering, and enable distribution**

48